7-16-2003

Trace Gas Measurements in Nascent, Aged, and Cloud-Processed Smoke from African Savanna Fires by Airborne Fourier Transform Infrared Spectroscopy (AFTIR)

Robert J. Yokelson
University of Montana - Missoula, bob.yokelson@umontana.edu

Issac T. Bertschi
University of Montana - Missoula

Ted J. Christian
University of Montana - Missoula

Peter V. Hobbs
University of Washington - Seattle Campus

Darold E. Ward
USDA Forest Service - Fires Sciences Laboratory

See next page for additional authors

Recommended Citation

Yokelson, R. J., I. T. Bertschi, T. J. Christian, P. V. Hobbs, D. E. Ward, and W. M. Hao, Trace gas measurements in nascent, aged, and cloud-processed smoke from African savanna fires by airborne Fourier transform infrared spectroscopy (AFTIR), J. Geophys. Res., 108(D13), 8478, doi:10.1029/2002JD002322, 2003.

Trace gas measurements in nascent, aged, and cloud-processed smoke from African savanna fires by airborne Fourier transform infrared spectroscopy (AFTIR)

Robert J. Yokelson,[1] Isaac T. Bertschi,[1,2] Ted J. Christian,[1] Peter V. Hobbs,[3] Darold E. Ward,[4,5] and Wei Min Hao[4]

Received 15 March 2002; revised 18 July 2002; accepted 16 December 2002; published 16 July 2003.

[1] We measured stable and reactive trace gases with an airborne Fourier transform infrared spectrometer (AFTIR) on the University of Washington Convair-580 research aircraft in August/September 2000 during the SAFARI 2000 dry season campaign in Southern Africa. The measurements included vertical profiles of CO_2, CO, H_2O, and CH_4 up to 5.5 km on six occasions above instrumented ground sites and below the TERRA satellite and ER-2 high-flying research aircraft. We also measured the trace gas emissions from 10 African savanna fires. Five of these fires featured extensive ground-based fuel characterization, and two were in the humid savanna ecosystem that accounts for most African biomass burning. The major constituents that we detected in nascent smoke were (in order of excess molar abundance) H_2O, CO_2, CO, CH_4, NO_2, NO, C_2H_4, CH_3COOH, HCHO, CH_3OH, HCN, NH_3, HCOOH, and C_2H_2. These are the first quantitative measurements of the initial emissions of oxygenated volatile organic compounds (OVOC), NH_3, and HCN from African savanna fires. On average, we measured 5.3 g/kg of OVOC and 3.6 g/kg of hydrocarbons (including CH_4) in the initial emissions from the fires. Thus, the OVOC will have profound, largely unexplored effects on tropical tropospheric chemistry. The HCN emission factor was only weakly dependent on fire type; the average value (0.53 g/kg) is about 20 times that of a previous recommendation. HCN may be useful as a tracer for savanna fires. $\Delta O_3/\Delta CO$ and $\Delta CH_3COOH/\Delta CO$ increased to as much as 9% in <1 h of photochemical processing downwind of fires. Direct measurements showed that cloud processing of smoke greatly reduced CH_3OH, NH_3, CH_3COOH, SO_2, and NO_2 levels, but significantly increased HCHO and NO. *INDEX TERMS:* 0320 Atmospheric Composition and Structure: Cloud physics and chemistry; 0345 Atmospheric Composition and Structure: Pollution—urban and regional (0305); 0368 Atmospheric Composition and Structure: Troposphere—constituent transport and chemistry; 0365 Atmospheric Composition and Structure: Troposphere—composition and chemistry; 0394 Atmospheric Composition and Structure: Instruments and techniques; *KEYWORDS:* biomass burning, savanna fires, oxygenated organic compounds, cloud chemistry, photochemistry, HCN

Citation: Yokelson, R. J., I. T. Bertschi, T. J. Christian, P. V. Hobbs, D. E. Ward, and W. M. Hao, Trace gas measurements in nascent, aged, and cloud-processed smoke from African savanna fires by airborne Fourier transform infrared spectroscopy (AFTIR), *J. Geophys. Res.*, *108*(D13), 8478, doi:10.1029/2002JD002322, 2003.

1. Introduction

[2] Biomass burning is a major source of trace gases for the global atmosphere [*Crutzen and Andreae*, 1990]. Savanna fires, occurring mostly in Africa, are the single largest type of biomass burning globally with domestic biofuel use second [*Andreae and Merlet*, 2001]. African savanna fires have been the focus of several major research campaigns including: FOS/DECAFE [*Lacaux et al.*, 1995], TRACE A [*Fishman et al.*, 1996], and SAFARI 92 [*Lindesay et al.*, 1996]. *Andreae* [1997] and *Andreae and Merlet* [2001] reviewed emissions measurements from these campaigns. In summary, previous work carried out mostly in southern Africa included: (1) Measurements of biomass consumption by fires in several savanna types ranging from "dry" savannas with "low" fire frequency (3–10 years) [*Trollope et al.*, 1996; *Stocks et al.*, 1996; *Shea et al.*, 1996] to "humid" savannas with high fire frequency (1–2 years) [*Shea et al.*, 1996; *Ward et al.*, 1996; *Hoffa et al.*, 1999].

[1]Department of Chemistry, University of Montana, Missoula, Montana, USA.
[2]Now at Interdisciplinary Arts and Sciences, University of Washington-Bothell, Bothell, Washington, USA.
[3]Department of Atmospheric Sciences, University of Washington, Seattle, Washington, USA.
[4]Fire Sciences Laboratory, USDA Forest Service, Missoula, Montana, USA.
[5]Now at Enviropyronics, LLC, White Salmon, Washington, USA.

0148-0227/03/2002JD002322

(Humid savannas have 700–1400 mm/yr of markedly seasonal rainfall and faster fuel buildup than dry savannas.) (2) Ground-based measurements of the initial emissions of CO_2, CO, and hydrocarbons [*Hao et al.*, 1996] and of CO_2, CO, and NO_x [*Lacaux et al.*, 1996] from fires in both humid and dry savannas. (3) Airborne measurements of the initial emissions from a "dry" savanna fire for CO_2, CO, CH_4, H_2, N_2O, and total nonmethane hydrocarbons [*Cofer et al.*, 1996] and CO_2, CO, NO_x, methyl halides, and some organic species [*Andreae et al.*, 1996]. (4) Measurements of haze layers and long range transport/photochemistry over southern Africa and the South Atlantic [*Swap et al.*, 1996; *Browell et al.*, 1996; *Talbot et al.*, 1996; *Singh et al.*, 1996] and interpretation of these measurements with models [*Jacob et al.*, 1996; *Thompson et al.*, 1996; *Chatfield et al.*, 1996; *Mauzerall et al.*, 1998]. A similar suite of savanna fires emissions was measured in West Africa in FOS/DECAFE [*Lacaux et al.*, 1995].

[3] Despite these accomplishments, many critically important gaps remained in our knowledge of African savanna fire emissions. For instance, there were no quantitative measurements, on any African fires, of the emissions of oxygenated volatile organic compounds (OVOC; alcohols, acids, aldehydes, etc.), even though OVOC were known to comprise about one-half of the organic emissions from fires in temperate and boreal ecosystems [*Yokelson et al.*, 1996, 1997, 1999; *Worden et al.*, 1997; *Holzinger et al.*, 1999; *Goode et al.*, 1999, 2000] and strongly influence smoke plume chemistry [*Mason et al.*, 2001]. There were almost no data on African fire emissions of important nitrogen-containing species such as HCN and NH_3. Earlier African measurements had focused either on "old" smoke of unknown (and probably mixed) ages in regional haze layers, or on nascent smoke (which we define as smoke $<\sim$5 min old) within a few kilometers of the flames. There was no explicit information on the transition between these two states. Also, most African fire measurements had been made in the dry savannas, forests, and plantations of South Africa rather than the humid savannas located north of 17°S where the vast majority of fires occur [*Justice et al.*, 1996]. Finally, there were very few data on emissions from the production and use of domestic biomass fuels.

[4] To help address these crucial gaps in knowledge, and as part of the Southern Africa Regional Science Initiative (SAFARI 2000: S2K), the University of Montana participated in both ground-based and airborne campaigns during the southern African dry season of 2000. The ground-based campaign focused on the trace gas emissions from the production and use of biofuels [*Bertschi et al.*, 2003a] and the unlofted emissions sometimes produced by prolonged smoldering combustion in wooded savannas [*Bertschi et al.*, 2003b]. In the airborne campaign we measured trace gases, mostly in smoke and haze from savanna fires, with an airborne Fourier transform infrared spetrometer (AFTIR) during 19 flights (>86 hours) between 14 August and 14 September aboard the University of Washington's (UW) Convair-580 research aircraft (UW Convair-580). The complete set of instruments for measuring trace gases and particles aboard the UW Convair-580 is described by *Sinha et al.* [2003a].

[5] In this paper we discuss some of the AFTIR trace gas measurements acquired on the UW Convair-580. In particular: (1) Vertical profiles of CO_2, CO, CH_4, and H_2O below 5.5 km in the regional haze layers that dominate southern Africa during the dry season due mostly to emissions from biomass burning. The profiles were measured above instrumented ground sites in association with overpasses by the NASA TERRA satellite and the ER-2. (2) The first broad characterization of the most abundant trace gases in nascent smoke from African savanna fires (i.e., including oxygen- and nitrogen-containing species). These measurements (which include fires in the humid savanna region) are used to calculate emission factors for savanna fires that can be used for regional emissions estimates. (3) Comparisons of nascent and downwind smoke samples of well-measured age reveal intriguing postemission changes in smoke composition due to photochemistry and cloud processing. This demonstrates the need to measure smoke less than a few moments in age to properly determine the "initial emissions" from fires and the value of measuring older smoke (of known age) to understand plume chemistry and characterize regional impacts. Plume chemistry links measurements in nascent smoke in the laboratory or field [e.g., *Lobert et al.*, 1991; *Hao et al.*, 1996; *Yokelson et al.*, 1996, 1999] with measurements in regional haze layers [e.g., *Talbot et al.*, 1996; *Blake et al.*, 1996].

2. Experimental Details

2.1. Measurement Strategy

[6] The AFTIR system is designed to obtain FTIR spectra of air flowing through, or detained within, a multipass cell inside an aircraft [*Yokelson et al.*, 1999; *Goode et al.*, 2000]. On the UW Convair-580, outside air samples were forced by ram pressure into a forward-facing inlet (25 mm internal diameter (i.d.)) with an opening 22 cm from the outer skin of the aircraft cabin roof. The air flowed next through 10 m of 25 mm i.d. Teflon bellows; a 16 liter, Pyrex, multipass cell; and $\sim$5 m of 25 mm i.d. tubing to a rear-facing outlet. Fast-acting valves (19 mm i.d.) on the inlet and outlet lines of the cell were used to temporarily trap the cell contents for signal averaging at desired times. In addition, closing the inlet and outlet valves reduced the noise in the 900–1100 cm^{-1} region of the AFTIR spectrum providing lower detection limits for many species [*Yokelson et al.*, 1999]. At the aircraft research speed (80 m/s) the flow rate through the system was $\sim$100 l/min. The $1/e$ decay time for a signal when exchanging the cell contents was 4–5 s, indicating a faster flow in the center of the cell where most of the optical path is located. The residence time in the exterior inlet tubing was only $\sim$2.5 ms. We further guarded against sampling artifacts by coating all the metal surfaces in the system with a nonreactive halocarbon wax [*Webster et al.*, 1994]. Recent tests in our laboratory showed that this wax imparts Teflon-like properties to metal surfaces [*Yokelson and Bertschi*, 2002].

[7] Infrared spectra of the cell contents were acquired continuously (every 0.83 s) throughout most of each flight and the flow-control valves were normally open, which flushed the cell with ambient air. To temporarily trap smoke plume "grab" samples we flew into the smoke plume and then closed the valves when the cell was well flushed with smoke. The valves remained closed for 1–3 min while several hundred spectra of the detained smoke sample were

acquired. The valves were then opened, which flushed the cell. Background grab samples were trapped at the same altitude just outside the plume and processed in the same way. We usually flushed the cell for one to many minutes before closing the valves for a smoke or background air sample. The low-noise spectra, acquired with the valves closed, were later averaged together (by sample) to further improve the signal-to-noise ratio.

[8] To measure initial emissions from a fire, we sampled smoke less than several minutes old by penetrating the rapidly rising column of smoke just above the flame front. "Aged" smoke samples were acquired within the plumes up to 30 km downwind. The age of downwind samples was computed from GPS and wind speed measurements. Vertical profiles of trace gases in regional haze layers, and in the free troposphere, were obtained by continuous sampling during rapid ascent/descent, or from a series of detained samples obtained during the horizontal legs of a "ladder" type flight profile.

2.2. Instrumental Details

[9] A detailed description of AFTIR and a schematic were given by *Yokelson et al.* [1999]. A brief, updated description follows. The system consisted of an infrared spectrometer (MIDAC, Inc.; resolution 0.5 cm^{-1}), a White cell (IR Analysis, Inc.), and optical components comounted on an aluminum, optical table (Newport, Inc.; 28 × 175 × 11 cm) that was shock mounted (Aeroflex, Inc) to the floor of the aircraft. The infrared beam exiting the spectrometer was directed by transfer optics to the "tripled" White cell. The beam made 120 passes of the 0.81 m basepath cell for a total path length of 97.5 m. After exiting the cell, the infrared beam was directed through a 25 mm focal length ZnSe lens onto a LN_2-cooled, MCT detector (Graseby, Inc., model FTIR M-16). Thermocouples were mounted inside each end of the cell and cell pressure was measured by a capacitive transducer (Type 626 MKS, Inc.). Pressure and temperature were stored at 1 Hz on the notebook computer that controlled and logged the AFTIR spectra. The total system weight was 133 kg.

2.3. Mixing Ratio Retrievals: Precision and Accuracy

[10] During S2K we recorded spectra of 264 "grab samples." Fifty-six samples were of biomass burning plumes, 5 of ship plumes [*Sinha et al.*, 2003b], and 203 of background air adjacent to plumes or in vertical profiles. We quantified the compounds responsible for all the major peaks in these spectra, which accounts for most of the trace gases present above 5–20 ppbv [*Goode et al.*, 1999]. Mixing ratios for H_2O, CO_2, and CH_4 were obtained by fitting sections of the transmission spectra of these samples with synthetic calibration classical least squares (CLS) methods [*Griffith*, 1996; *Yokelson et al.*, 1996, 1997; *Yokelson and Bertschi*, 2002]. The CO mixing ratios were obtained from a deployment-specific, mathematical interpolation based on a large set of pre- and postexperiment calibration spectra that spanned the relevant temperatures, pressures, and mixing ratios. Excess mixing ratios in smoke (ΔX) were assumed to be the mixing ratio of a species "X" in smoke minus the mixing ratio of X in the closest sample of background air. Absorbance spectra of smoke were generated using background-sample spectra collected nearby at the same altitude. Excess mixing ratios in smoke were obtained directly from the smoke-absorbance spectra using synthetic-calibration CLS methods for NO, NO_2, and formaldehyde (HCHO). Excess mixing ratios for H_2O, formic acid (HCOOH), acetic acid (CH_3COOH), ethylene (C_2H_4), acetylene (C_2H_2), hydrogen cyanide (HCN), methanol (CH_3OH), and ozone (O_3) were retrieved from the absorbance spectra by spectral subtraction [*Yokelson et al.*, 1997].

[11] One sample of background air was retained and remeasured 23 and 27 min later to test the precision of the AFTIR mixing ratios. The standard deviation/average was CO_2 (0.11%, 0.46 ppm), CO (0.63%, 0.9 ppb), and CH_4 (0.77%, 14 ppb). The detection limits varied by spectrum depending mostly on the amount of signal averaging or H_2O concentration. For most compounds the detection limit was usually 5–10 ppbv, but for NO_x, formaldehyde, acetic acid, and ozone it was usually closer to 15–20 ppbv. The typical absolute uncertainty in the excess mixing ratios is estimated to be ±5% (1σ), or the detection limit, whichever is larger. The accuracy, as determined by testing with calibration standards, for several molecules was: CO_2, CO and CH_4 (1–2%); NO, NO_2, and CH_3OH (1–5%); and NH_3 (variable as discussed below). The CO values obtained by AFTIR were not significantly different from those obtained on a nearby aircraft using a CMDL flask-sampling system [*McMillan et al.*, 2003].

[12] NH_3 was the only compound affected by brief storage in the cell. The spectra acquired during storage were analyzed at 0.83 s resolution and the NH_3 mixing ratios at the beginning of the storage periods were obtained from the NH_3 decay profiles. Laboratory tests with a wide variety of gases (acetic acid, methanol, NO_x, etc), carried out just before the S2K flights (Yokelson et al., in preparation), showed that AFTIR could have additional, variable losses (0–50%) for NH_3 only, which result from passivation of the Pyrex cell during sample acquisition. The NH_3 losses were negligible when the cell was exposed to the sample for longer times before closing the valves (30 s) or when several smoke samples were taken consecutively. Larger losses occurred when very short "cell exposure times" were used (3–4 s). During S2K we minimized passivation losses by using long cell exposure times and sometimes acquiring consecutive smoke samples. We estimate that the NH_3 values reported here are 5–20% low on the average.

3. Results and Discussion

3.1. Typical Trace Gas Profiles for the Southern African Dry Season Troposphere

[13] To provide a context for this study, we describe a few typical trace gas profiles up to 5.5 km during S2K. (The location of many vertical profiles is given by *Sinha et al.* [2003a] and one profile is discussed by *McMillan et al.* [2003].) Most of southern Africa was dominated during the dry season of 2000 by a well-mixed haze layer that extended to 3–6 km in altitude and contained aged emissions from savanna fires, cooking fires, vegetation and industry. This layer was characterized by low visibility and high levels of O_3 (30–100 ppbv), CO (200–650 ppbv), and water (<10,000 ppm). At the top of the haze layer there was usually a transition (~0.2 km thick) to the free tropo-

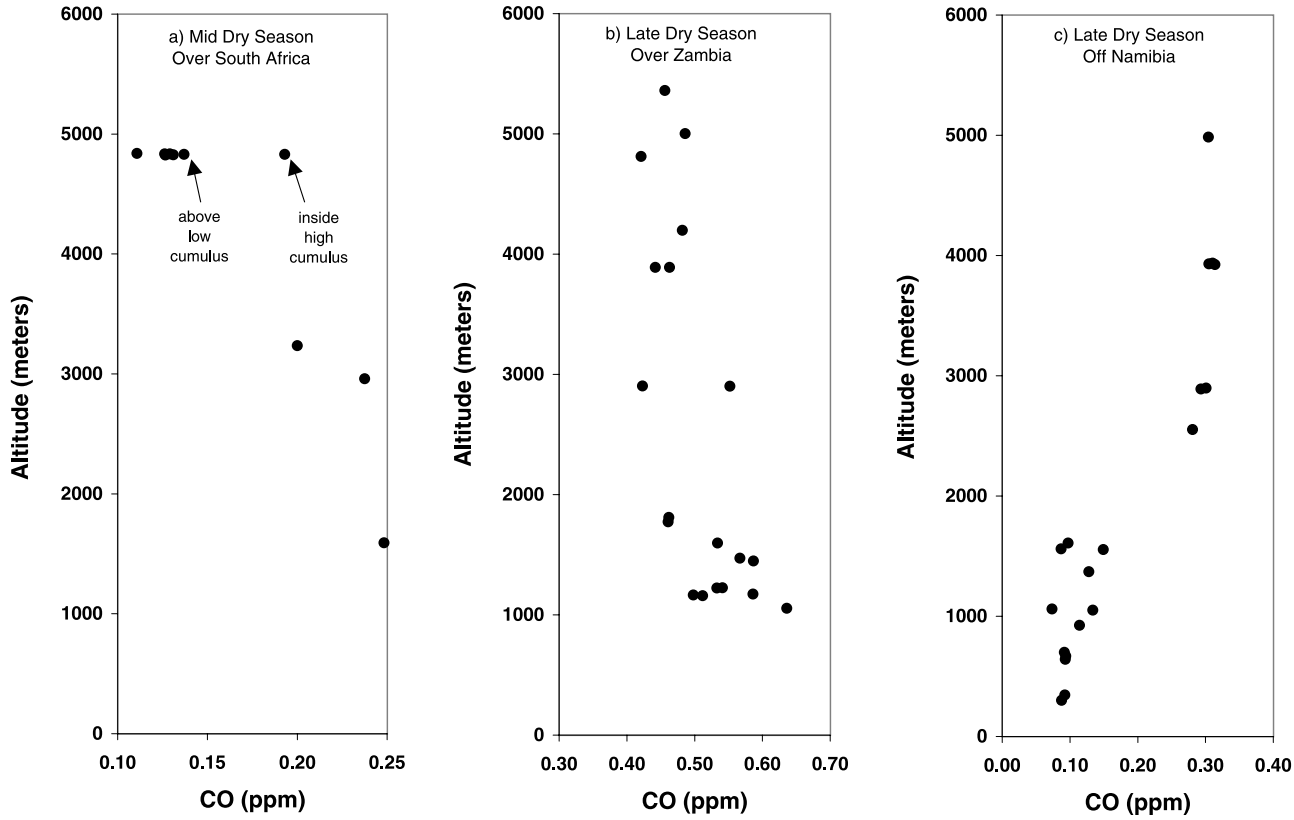

Figure 1. Examples of CO mixing ratios measured with AFTIR well away from distinct smoke plumes. a) 23 August 2000 (mid dry season) over Pietersburg, South Africa, well south of most fire activity. A well-mixed haze layer extended to ~3.5 km with much cleaner, drier air above. The data points obtained above or within nonprecipitating cumulus show mixing of the layers by cloud-related convection. b) Above the airport in Mongu, Zambia on 6 September 2000 (late dry season) in the humid savanna region where most fires occur. The CO values are much greater and show that the haze layer extended to above 5.5 km. c) Over the South Atlantic Ocean off Namibia on 13 September 2000 (late dry season) showing the continental outflow above 2.4 km. The profile is inverted when compared to the situation in a) and the O_3 was 40 ppbv higher in the outflow layer than in the clean, maritime layer. Multiple values at the same altitude are from samples at different times and/or locations.

sphere, which had much lower levels of CO (<120 ppb) and H_2O (<500 ppm). Especially in the humid savanna region it was common to observe many small fires burning within a 10–20 km radius. Very few savanna fire plumes penetrated the top of the well-mixed haze layer. Thus, as the nascent smoke from fires aged it was diluted by the background haze and it faded into the haze layer within 10–30 km downwind of the fire. The vertical profiles away from distinct plumes can be classified into the three categories illustrated in Figure 1.

[14] Figure 1a shows a few AFTIR, CO mixing ratios obtained on 23 August (UW Flight 1821) over Pietersburg, South Africa that reflect a typical vertical profile over South Africa (which is well south of most of the fire activity) during the mid dry season. In these profiles, the well-mixed layer extended to ~3.5–3.7 km and it was topped by much cleaner, drier air. In some cases, a shallow clean layer was found near this altitude sandwiched between layers of dirty air [*Hobbs*, 2003]. The sparse data from flight 1821 are shown here, because they also demonstrate some interesting effects of cumulus convection. During a level flight leg in the clean, dry free troposphere at ~4.8 km we encountered strongly elevated water vapor and modestly elevated CO above nonprecipitating cumulus clouds (as indicated). Other effects measured above these clouds, by UW instruments, were increased upwelling uv and decreased O_3. As also shown in Figure 1a, when we penetrated the interior of a taller cumulus cloud at 4.8 km, both CO and $H_2O_{(g)}$ increased to values measured in the haze layer ~2 km below. These observations show that convection in nonprecipitating cumulus can enhance mixing between atmospheric layers. Clouds such as these were common during the 2000 dry season and did not produce rain that could have diminished biomass burning. Thus, convection could be an important regional mechanism for the long-range transport of smoke that would otherwise be confined to the well-mixed layer [*Hobbs*, 2003]. However, as discussed in section 3.3.2, even a brief residence time in clouds can cause large changes in the chemical composition of smoke. Thus, it is important to know the amount of African smoke that is both elevated and modified by passage through a "cloud gateway." Cloud effects on smoke may be even more important in Brazil and Southeast Asia where dry season clouds are more common [*Reid et al.*, 1998].

[15] A second type of vertical profile is illustrated by the AFTIR CO mixing ratios obtained over Mongu, Zambia on 6 September (UW Flight 1832, Figure 1b). This type of profile was commonly observed in the final third of the 2000 dry season over or near the humid savanna, which featured much more intense biomass burning. As a result the CO mixing ratios were much higher and the mixed haze layer extended to a much greater altitude. On this particular day, the Cloud Physics Lidar onboard the ER-2 indicated that the haze layer extended to ~6 km [*Schmid et al.*, 2003]. This deeper, more concentrated haze covered vast regions of southern Africa north of 20°S. Satellite images of the distribution of African fires suggest that such haze might have extended as far north as the equator [*Cahoon et al.*, 1992].

[16] Finally, in Figure 1c, we show the AFTIR CO profile obtained off the Namibia coast on 13 September (UW Flight 1837). Clean marine air with low CO was found near the surface and high CO was observed above ~2.4 km. Backward trajectories indicate that the lower, clean air was transported from much further south over the Atlantic, and that the upper-level haze was continental outflow that had passed through the active burning region 2–4 days previously (HYSPLIT4 (Hybrid Single-Particle Lagrangian Integrated Trajectory) Model, 1997. Web address: http://www.arl.noaa.gov/ready/hysplit4.html, NOAA Air Resources Laboratory, Silver Spring, MD). There was a sharp increase of 40 ppbv in the AFTIR ozone on entering the continental outflow from below, probably due to photochemical processing of fire emissions. Photochemistry in this aged haze layer may be enhanced because it is often located above a layer of reflective, low elevation marine clouds. The continental outflow (studied in SAFARI 92 and TRACE A) is another avenue for transport/processing of biomass burning emissions in addition to clouds.

3.2. Major Trace Gases Emitted by African Savanna Fires

3.2.1. Fire Descriptions

[17] We describe key features of the 10 savanna fires sampled in this study. We sampled three fires of opportunity in grassland, with some brush and small trees, in southern Kruger National Park near Skukuza, South Africa during UW Flights 1815 and 1822. We sampled two other fires of opportunity on UW Flight 1825. One was in a coastal lowland, open forest with a grass/brush understory, located ~100 km south of Beira, Mozambique. We also obtained a single, high elevation sample of a 3.4 km tall, vertical smoke column above the Lebombo Mountains of Mozambique. This smoke may have been processed by a capping cumulus cloud that dissipated before our arrival. We do not know the fuel type for this fire. The other five fires were planned burns and the airborne sampling was carried out in close coordination with ground-based teams. Two large prescribed fires were sampled in the Madikwe Game Reserve in the Limpopo River valley (UW Flights 1816 and 1819). These fires burned in nearly pure grassland with only a few scattered small bushes. The first of these fires produced a 3.4 km tall, vertical smoke column with a large capping cumulus cloud that allowed sampling of cloud-processed smoke. We sampled a large (1000 ha) prescribed fire in the Timbavati Game Reserve (adjacent to Kruger National Park) on 7 September (UW flight 1834). During this fire we carried out extensive downwind sampling [*Hobbs et al.*, 2003]. The fuel consumption and fire behavior for the prescribed burns at Madikwe and Timbavati were measured by T. Landmann personal communication, 2002).

[18] We also sampled two planned fires in the humid savannas of Zambia. Both fires were burned in the traditional manner by local crews. The fuel consumption and fire behavior were measured by J. Pereira (personal communication, 2002). The first of these fires was in miombo woodland (1 September, UW Flight 1826). Miombo woodland can be classified as humid (wooded) savanna or tropical dry forest. Central Africa has 2.8 million km^2 of miombo, which comprises the largest contiguous ecosystem of this type on Earth [*Desanker et al.*, 1997]. The miombo understory (mostly grass and leaf litter) burns about every two years [*Shea et al.*, 1996; *Desanker et al.*, 1997] and this likely accounts for more biomass burning than any other single ecosystem on Earth [*Desanker et al.*, 1997]. The miombo covers much of central Africa (~80% of Zambia is miombo [*Hoffa et al.*, 1999]) and fires in the miombo account for the great majority of sub-Sahelian fires [*Justice et al.*, 1996; *Desanker et al.*, 1997]. Therefore, this planned fire likely represents the most common type of African savanna fire. The other planned fire in Zambia (5 September, UW Flight 1831) was in a dambo. Dambos are seasonally flooded grasslands that are the major enclaves in the miombo. Most dambos burn annually [*Hoffa et al.*, 1999], which accounts for a large fraction of African fires.

3.2.2. Excess Mixing Ratios Measured in Biomass Burning Plumes

[19] Most gases (exceptions include N_2, H_2, and some sulfur compounds [*Goode et al.*, 1999]) can be detected by FTIR when they are present at mixing ratios >5–20 ppbv. In the AFTIR smoke spectra acquired in this study all the major features were due to H_2O, O_3, CO_2, CO, CH_4, C_2H_4, C_2H_2, HCHO, CH_3OH, HCOOH, CH_3COOH, NO, NO_2, NH_3, and HCN. Thus, these compounds are 15 of the most abundant compounds in smoke. In Table 1 we show the excess mixing ratios obtained in samples of distinct biomass-burning plumes along with fire name, UW flight number, date, and the UTC time (local time = UTC + 2 hr), longitude, latitude, and altitude of the sample. Each sample has a brief descriptive comment, which indicates when samples were obtained downwind from the source or had undergone cloud processing. In some of the more dilute samples the excess mixing ratios of some compounds were "reasonable," but below our estimated detection limit of 5 ppbv so they were omitted from Table 1. Note also the much higher levels of CO encountered in nascent plumes (up to ~11 ppm) than in the background haze (Figure 1).

3.2.3. Estimation of Fire-Average, Initial Emission Ratios

[20] We estimated fire-average, initial emission ratios (ER) between compounds from the slope of the least squares line, with the intercept forced to zero, in a plot of one set of excess mixing ratios versus another [*Yokelson et al.* 1999]. We omitted any samples that were affected by photochemistry or cloud processing from our emission ratio plots to determine initial emission ratios. Two examples of these plots are shown in Figure 2. Omitting the excess mixing ratios below 5 ppb reduced the correlation coeffi-

Table 1. Sample Type, Location, Time, and Excess Mixing Ratios (>0.005 ppm) for AFTIR Measurements in African Biomass Burning Plumes During SAFARI 2000

Sample Description	Altitude, masl	Latitude, °	Longitude, °	Time, UTC	CO_2, Δppmv	CO, Δppmv	CH_4, Δppmv	O_3, Δppmv	C_2H_4, Δppmv	C_2H_2, Δppmv	HCHO, Δppmv	CH_3OH, Δppmv	HAc,[a] Δppmv	HCO_2H, Δppmv	NH_3, Δppmv	NO, Δppmv	NO_2, Δppmv	HCN, Δppmv
Excess Mixing Ratios for the Compounds Detected in Smoke Directly Above Two Fires Near Skukuza (SA) (17 August 2000; UW Flight 1815)																		
Smoldering fire no. 1	1255	−25.463	31.604	0944:27	0.6	0.031			0.006					0.016				
Repeat	865	−25.454	31.567	0953:57	11.1	0.569	0.049		0.014		0.013	0.010	0.006				0.020	0.007
Repeat	884	−25.454	31.576	1002:11	8.9	0.612	0.058		0.015		0.014	0.012	0.019	0.006	0.031		0.022	
"Dark brown" haze	2036	−25.279	31.394	1040:02	11.1	0.100	0.023											
Repeat	2057	−25.298	31.380	1046:47	7.6	0.089												
Flaming fire no. 2	1124	−24.466	31.830	1104:48	60.3	8.892	0.527	−0.023	0.159	0.021	0.131	0.137	0.192	0.020	0.048	0.032	0.124	0.070
Repeat	1160	−24.468	31.839	1109:10	163.1	11.510	0.688	−0.034	0.228	0.044	0.200	0.159	0.204	0.024	0.104	0.158	0.248	0.118
Repeat	1084	−24.457	31.837	1126:13	67.8	4.940	0.279	−0.030	0.099	0.018	0.053	0.066	0.096	0.010	0.031	0.055	0.133	0.048
Excess Mixing Ratios for the Compounds Detected in Smoke Directly Above the Fire and in Cloud-Processed Smoke at Madikwe (SA) (18 August 2000; UW Flight 1816)																		
Nascent smoke	1084	−24.695	26.445	0915:00	34.4	5.917	0.417		0.084	0.015	0.054	0.101	0.094	0.042	0.053	0.024	0.097	0.040
Repeat	1129	−24.659	26.431	0920:26	80.0	3.364	0.196	−0.037	0.062	0.015	0.048	0.053	0.042	0.038		0.120	0.138	0.041
Repeat	1163	−24.652	26.447	0932:58	16.8	1.059	0.123	−0.022	0.009			0.016	0.012	0.012		0.037	0.033	
Weak sample	1692	−24.838	26.327	0955:52	6.2	0.029	0.016											
Nascent smoke below cumulus	1945	−24.620	26.300	1222:46	92.5	5.043	0.136	−0.073	0.071	0.027	0.102	0.068	0.102	0.018	0.054	0.185	0.191	0.064
Cloud-processed smoke	3866	−24.669	26.301	1234:07	41.4	2.663	0.071		0.047	0.005	0.059	0.015	0.050	0.014		0.122	0.086	0.046
More intense cloud processing	4166	−24.597	26.359	1239:12	35.1	2.215	0.095		0.036		0.076		0.022	0.011		0.121	0.058	0.039
Excess Mixing Ratios for the Compounds Detected in Smoke Directly Above the Fire at Madikwe (SA) (20 August 2000; UW Flight 1819)																		
Near plume base	1373	−24.788	26.264	1302:17	61.8	2.394	0.130		0.036	0.019	0.043	0.037	0.036	0.021		0.040	0.078	0.034
Repeat	1363	−24.785	26.270	1302:29	22.0	1.060	0.080	−0.020	0.016		0.042	0.021		0.008		0.037	0.053	0.015
Repeat	1390	−24.713	26.192	1310:41	54.1	2.964	0.115	−0.063	0.063	0.014	0.071	0.042	0.057	0.024		0.054	0.160	0.044
Repeat	1616	−24.675	26.322	1327:10	104.6	4.557	0.202	−0.061	0.097	0.023	0.103	0.066	0.070	0.044		0.113	0.228	0.058
Repeat	1340	−24.737	26.295	1352:01	34.8	2.374	0.101		0.046	0.012	0.050	0.038	0.049	0.015	0.029	0.021	0.108	0.025
Excess Mixing Ratios for the Compounds Detected in Smoke Directly Above the Fire Near Skukuza (SA) (29 August 2000; UW Flight 1824)																		
Nascent smoke	712	−25.133	31.401	1412:55	27.4	2.032	0.143		0.033	0.010	0.014	0.039	0.042	0.006		0.028	0.070	0.006
Repeat	761	−25.145	31.401	1420:47	69.7	5.042	0.355		0.078	0.021	0.055	0.103	0.082	0.029	0.016	0.080	0.128	0.032
Excess Mixing Ratios for the Compounds Detected in Smoke Directly Above and Downwind From a Fire 100 km South of Beira, Mozambique (31 August 2000; UW Flight 1825)																		
Smoke at source	263	−20.972	34.697	1120:03	53.8	4.852	0.296		0.089	0.020	0.069	0.064	0.068	0.028			0.137	0.030
Repeat	217	−20.973	34.699	1126:07	60.2	6.734	0.415	−0.016	0.098	0.022	0.076	0.099	0.104	0.021			0.192	0.034
Repeat	213	−20.976	34.701	1134:20	38.6	3.233	0.177		0.043	0.016	0.047	0.034	0.084	0.026			0.138	0.018
19.5 km downwind	176	−21.147	34.668	1144:14	2.1	0.290	0.029	0.021					0.007	0.009			0.036	
19.9 km downwind	200	−21.149	34.646	1200:15	3.9	0.314	0.021	0.017					0.018	0.006				
19.2 km downwind	347	−21.143	34.652	1220:48	2.5	0.348	0.015						0.032	0.011				
26.4 km downwind	332	−21.205	34.628	1223:55	1.3	0.334	0.017	0.028					0.013	0.007				
Excess Mixing Ratios for the Single Sample of a Plume Penetrating the Haze Layer Over the Northern Lebombo Mountains, Mozambique (31 August 2000; UW Flight 1825)																		
Smoke above haze layer	3874	−23.394	31.846	1328:49	38.9	3.286	0.046		0.057		0.081	0.023	0.043	0.036		0.076	0.059	
Excess Mixing Ratios for the Compounds Detected in Smoke Above and Near the Miombo Fire Near Kaoma, Zambia (1 September 2000; UW Flight 1826)																		
Ignition 0856 UTC; first source sample	1340	−14.798	24.487	0857:17	28.5	1.971	0.083	−0.037	0.032	0.007	0.029	0.027	0.045		0.035	0.020	0.070	0.016
Repeat; UW bag 1; Terra overpass	1332	−14.822	24.478	0901:46	43.0	4.929	0.217	−0.062	0.051	0.014	0.052	0.074	0.084	0.018	0.080	0.060	0.097	0.026

[a] HAc = acetic acid.

Table 1. (continued)

Sample Description	Altitude, masl	Latitude, °	Longitude, °	Time, UTC	CO_2, Δppmv	CO, Δppmv	CH_4, Δppmv	O_3, Δppmv	C_2H_4, Δppmv	C_2H_2, Δppmv	HCHO, Δppmv	CH_3OH, Δppmv	HAc,[a] Δppmv	HCO_2H, Δppmv	NH_3, Δppmv	NO, Δppmv	NO_2, Δppmv	HCN, Δppmv
3rd source sample	1248	−14.814	24.477	0909:04	95.4	5.109	0.164	−0.079	0.062	0.022	0.052	0.062	0.071	0.027	0.028	0.099	0.167	0.033
Repeat; UW bag 2	1330	−14.829	24.482	0919:18	59.6	3.698	0.113	−0.061	0.045	0.015	0.029	0.043	0.031	0.025	0.017	0.056	0.131	0.015
5th source sample; top of plume	1905	−14.817	24.461	0926:36	30.1	1.506	0.044	−0.038	0.026		0.018	0.021	0.036	0.007	0.004		0.060	
8 km downwind, smoke from two fires	1976	−14.822	24.364	0938:49	2.9	0.276	0.015						0.018		0.012			
Excess Mixing Ratios for the Compounds Detected in Smoke Directly Above the Dambo Fire Near Kaoma, Zambia (5 September 2000; UW Flight 1831)																		
Ignition 1149 UTC, sample no. 1	1308	−14.824	24.453	1155:18	50.9	4.222	0.111	−0.021	0.071	0.018	0.026	0.044	0.077	0.031		0.027	0.120	0.021
Sample no. 2	1342	−14.813	24.455	1157:29	81.9	3.593	0.100	−0.048	0.070	0.022	0.068	0.036	0.065	0.037		0.028	0.147	0.021
Sample no. 3	1353	−14.804	24.459	1202:18	194.0	4.489	0.198	−0.100	0.117	0.039	0.028	0.041	0.049	0.038		0.135	0.216	0.061
Sample no. 4	1368	−14.823	24.448	1204:36	308.2	7.673	0.314	−0.100	0.191	0.060	0.112	0.067	0.077	0.068		0.318	0.307	0.097
Sample no. 5, fire almost over	1351	−14.808	24.450	1232:50	18.2	0.741	0.013	−0.028	0.011			0.013		0.010		0.017	0.038	
Excess Mixing Ratios for the Compounds Detected in Smoke Above and Downwind From the Prescribed Fire at Timbavati, South Africa (7 September 2000; UW Flight 1834)																		
Ignition 0801 UTC, TERRA 0828 UTC, ER2 0829 UTC, Source sample no. 1, UW bag no. 1	601	−24.373	31.257	0842:47	79.2	5.738	0.345	−0.052	0.091	0.019	0.109	0.086	0.075	0.033	0.005	0.057	0.137	0.037
Source sample no. 2	837	−24.371	31.240	0846:11	68.6	4.024	0.214	−0.052	0.058	0.014	0.074	0.055	0.058	0.033	0.013	0.052	0.123	0.029
9 km downwind	643	−24.290	31.269	0855:10	19.1	1.776	0.109	0.022	0.021	0.006	0.016	0.028	0.014	0.017			0.051	0.018
Source sample no. 3, UW bag no. 3	1005	−24.358	31.229	0921:26	6.9	0.911	0.080	−0.012	0.012		0.020	0.020	0.023					0.009
16 km downwind	1615	−24.235	31.280	0932:58	13.9	1.042	0.055	0.060	0.031		0.031	0.010	0.030	0.011		0.033		0.008
18 km downwind	1547	−24.215	31.207	0934:22	21.3	1.625	0.117	0.098	0.044		0.037		0.071					0.018
20 km downwind, UW bag no. 4	1570	−24.194	31.213	0939:51	10.1	0.954	0.060	0.086	0.029		0.031	0.007	0.036	0.005				0.011
Source sample no. 4	659	−24.356	31.248	0945:53	15.6	1.592	0.067		0.020		0.025	0.019	0.053	0.006			0.051	
5 km downwind	656	−24.340	31.224	0950:53	3.3	0.459	0.026											
17 km downwind	587	−24.232	31.150	0953:39	8.9	0.629	0.039											
27 km downwind	585	−24.142	31.122	0956:50	6.6	0.485												
24 km downwind	632	−24.177	31.088	1014:42	6.1	0.549	0.033	0.031			0.010		0.027				0.006	
25 km downwind, UW bag no. 5	523	−24.165	31.094	1020:31	6.3	0.644	0.028	0.054			0.010	0.009	0.035					
28 km downwind	605	−24.145	31.077	1036:21	7.1	0.426	0.021	0.019			0.020	0.005	0.032					

masl, meters above sea level.

[a]HAc is an abbreviation for acetic acid.

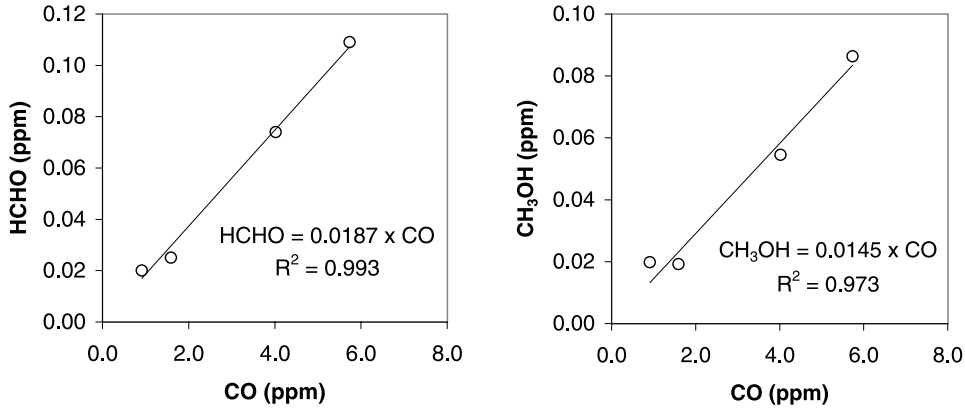

Figure 2. Fire-average, initial emission ratios for each compound are estimated for each fire from the slope of the regression line in a plot of the compound's excess mixing ratios versus the simultaneously measured excess mixing ratios of CO or CO_2. The two examples here (out of >100) show how ΔHCHO/ΔCO and $\Delta CH_3OH/\Delta CO$ were derived for all AFTIR samples obtained in smoke from the Timbavati Fire (UW Flight 1834) that was less than a few minutes old.

cient (R^2) for a few plots, but never affected the slope. We list the emission ratios (as determined from the slopes) for each fire and compound in Table 2. We sampled two fires in similar fuels near Skukuza on flight 1815, which we treated as one fire in the emission ratio plots and in Table 2.

3.2.4. Estimation of Fire-Average, Initial Emission Factors

[21] We estimated fire-average, initial emission factors (EF) for each observed trace gas from our fire-average, initial emission ratios using the carbon mass balance method [*Ward and Radke*, 1993] as described by *Yokelson et al.* [1999]. In brief, we assume that all the volatilized carbon is detected and that the fuel carbon content is known. By ignoring particulate and unmeasured gases we are probably inflating the emission factors by 1–2% [*Andreae and Merlet*, 2001]. We acquired two samples each of dambo grass and miombo litter, which are the major fuel components for humid savanna fires [*Shea et al.*, 1996]. We measured average carbon contents for these fuel types of 47.9 and 53.7%, respectively. Thus we assumed in our EF calculations that all the fires burned in fuels containing 50% carbon by mass. This is in good agreement with previous studies of tropical biomass [*Susott et al.*, 1996], but the actual fuel carbon percentage may vary by ±10% (2σ). We also calculated the fire-average modified combustion efficiency (MCE, $\Delta CO_2/(\Delta CO_2 + \Delta CO)$) for each fire using the fire-average $\Delta CO/\Delta CO_2$ emission ratio and the equation $MCE = 1/((\Delta CO/\Delta CO_2) + 1)$ [*Ward and Radke*, 1993]. MCE is useful as an index of the relative amount of flaming and smoldering combustion throughout a fire. The fire-average, initial emission factors for each compound and fire, along with the fire average MCE, are listed in Table 2. Because NO is mostly converted to NO_2 within minutes of emission (largely due to reaction with O_3 in the entrained background air), we report a single EF for "NO_x as NO." Our EF (and ER) values are also shown by *Sinha et al.* [2003a] to facilitate integration/comparison with EF (and ER) measured by other instruments on the Convair-580 using independent sampling strategies. In Figure 3 we plot the emission factors for each smoldering compound we detected (except CO) versus MCE [*Yokelson et al.*, 1996]. This gives some idea of the natural gradient in emission factors that results from savanna fires burning under a range of vegetative/environmental conditions and, therefore, with different mixtures of flaming and smoldering combustion.

3.2.5. How Well Do Our ER and EF Values Represent African Savanna Fires?

[22] A number of factors suggest that the values shown in Table 2 are representative of African savanna fires in general. For example, the measurements include the humid savanna region, which dominates the total burning and they were made in the middle-late dry season when measured smoke levels in this region peak [*Eck et al.*, 2003]. In addition, we sampled as much of the lifetime of the plumes as possible, especially for the planned fires. Also, when samples from the same fire clearly reflected different relative amounts of flaming and smoldering, they were all included in the emission ratio plots, even if the R^2 of the plot was diminished. (In theory, the separate measurements of mostly flaming and mostly smoldering combustion could also be used to scale the measurements to other scenarios where different MCE are appropriate.)

[23] There are some fundamental limits to what our data can represent. One limitation is due to the timing of S2K. *Hoffa et al.* [1999] found that some early dry season fires in the humid savanna region can burn with lower MCE and thus they may have relatively higher emission factors for smoldering compounds. This suggests that the regression equations in Figure 3 should be used to calculate EF at lower MCE to explicitly estimate emissions from these fires.

[24] Another limitation involves smoke that is produced by a fire, but not entrained into a convection column where it can be sampled by an aircraft. This type of smoke results from "residual smoldering combustion" (RSC) [*Bertschi et al.*, 2003b]. Following Bertschi et al. we can estimate the correction due to RSC for the EF measured from an aircraft using the expression:

$$EF_{actual} = EF_{RSC} * F_{RSC} + EF_{AB} * F_{AB} \quad (1)$$

where EF_{actual} is the true fire-average emission factor, EF_{RSC} the emission factor during RSC, F_{RSC} the fraction of

Table 2. Initial Emission Ratios (ER) and Emission Factors (EF)[a] for Fires Investigated by AFTIR on the UW Convair-580 Aircraft During SAFARI 2000

UW Flight Number	1815	1816	1819	1824	1825	1825	1826	1831	1834			
Date (2000)	17 August	18 August	20 August	29 August	31 August	31 August	1 September	5 September	7 September	Study		Humid Savanna
Fire Location/Name	Skukuza1, 2	Madikwe1	Madikwe2	Kruger	Beira	Lebombo[b]	Miombo	Dambo	Timbavati	Average	1σ	Average[c]
CO_2 EF	1678	1715	1738	1688	1643	1675	1711	1779	1696	1703	39	1734
CO/CO_2 ER	0.0784	0.0590	0.0460	0.0726	0.0989	0.0845	0.0630	0.0264	0.0692	0.0664	0.0214	0.0508
CO EF	83.7	64.4	50.9	78.0	103.4	90.0	68.6	29.9	74.7	71.5	21.7	55.7
MCE	0.927	0.944	0.956	0.932	0.910	0.922	0.941	0.974	0.935	0.938	0.019	0.952
NO/CO_2 ER	0.0009	0.0019	0.0010	0.0011		0.0020	0.0010	0.0009	0.0008	0.0011	0.0004	0.0010
NO_2/CO_2 ER	0.0016	0.0020	0.0022	0.0019	0.0030	0.0015	0.0020	0.0011	0.0018	0.0020	0.0005	0.0017
NO_x as NO EF	2.86	4.56	3.79	3.45	3.36	3.97	3.50	2.43	3.01	3.37	0.64	3.14
CH_4/CO ER	0.0594	0.0541	0.0483	0.0704	0.0606	0.0141	0.0364	0.0375	0.0583	0.0531	0.0118	0.0368
CH_4 EF	2.84	1.99	1.40	3.14	3.58	0.73	1.43	0.64	2.49	2.19	1.00	1.16
C_2H_4/CO ER	0.0192	0.0151	0.0200	0.0156	0.0155	0.0174	0.0119	0.0231	0.0160	0.0171	0.0033	0.0156
C_2H_4 EF	1.61	0.97	1.02	1.22	1.60	1.57	0.82	0.69	1.19	1.19	0.35	0.77
C_2H_2/CO ER	0.0033	0.0037	0.0054	0.0043	0.0037		0.0037	0.0072	0.0034	0.0043	0.0013	0.0049
C_2H_2 EF	0.26	0.22	0.26	0.31	0.36		0.24	0.20	0.24	0.26	0.05	0.22
HCHO/CO ER	0.0158	0.0139	0.0225	0.0104	0.0126	0.0246	0.0102	0.0122	0.0187	0.0145	0.0043	0.0109
HCHO EF	1.42	0.96	1.23	0.87	1.40	2.37	0.75	0.39	1.50	1.06	0.39	0.63
CH_3OH/CO ER	0.0143	0.0156	0.0148	0.0202	0.0136	0.0071	0.0131	0.0093	0.0145	0.0144	0.0030	0.0118
CH_3OH EF	1.37	1.15	0.86	1.80	1.61		1.03	0.32	1.24	1.17	0.46	0.79
CH_3COOH/CO ER	0.0192	0.0168	0.0169	0.0169	0.0164	0.0132	0.0148	0.0125	0.0146	0.0160	0.0020	0.0140
CH_3COOH EF	3.44	2.32	1.84	2.82	3.64	2.55	2.18	0.80	2.34	2.42	0.90	1.72
HCOOH/CO ER	0.0021	0.0066	0.0087	0.0054	0.0045	0.0108	0.0051	0.0087	0.0064	0.0059	0.0022	0.0063
HCOOH EF	0.29	0.70	0.73	0.69	0.76	1.60	0.57	0.43	0.79	0.62	0.18	0.53
NH_3/CO ER	0.0076	0.0081	0.0122	0.0027			0.0097		0.0016	0.0070	0.0041	0.0065
NH_3 EF	0.39	0.32	0.38	0.13			0.40		0.07	0.28	0.14	0.27
HCN/CO ER	0.0094	0.0108	0.0131	0.0059	0.0055		0.0056	0.0108	0.0072	0.0085	0.0029	0.0073
HCN EF	0.76	0.67	0.64	0.44	0.55		0.37	0.31	0.52	0.53	0.15	0.35

[a]Emission factors are expressed as g/kg.

[b]Since for this fire, the vegetation is unknown, CH_4 is unreliable, and the NO_x and oxygenated compounds were influenced by cloud processing, the data for these compounds from this fire are not included in the study-average values.

[c]See section 3.2.6.

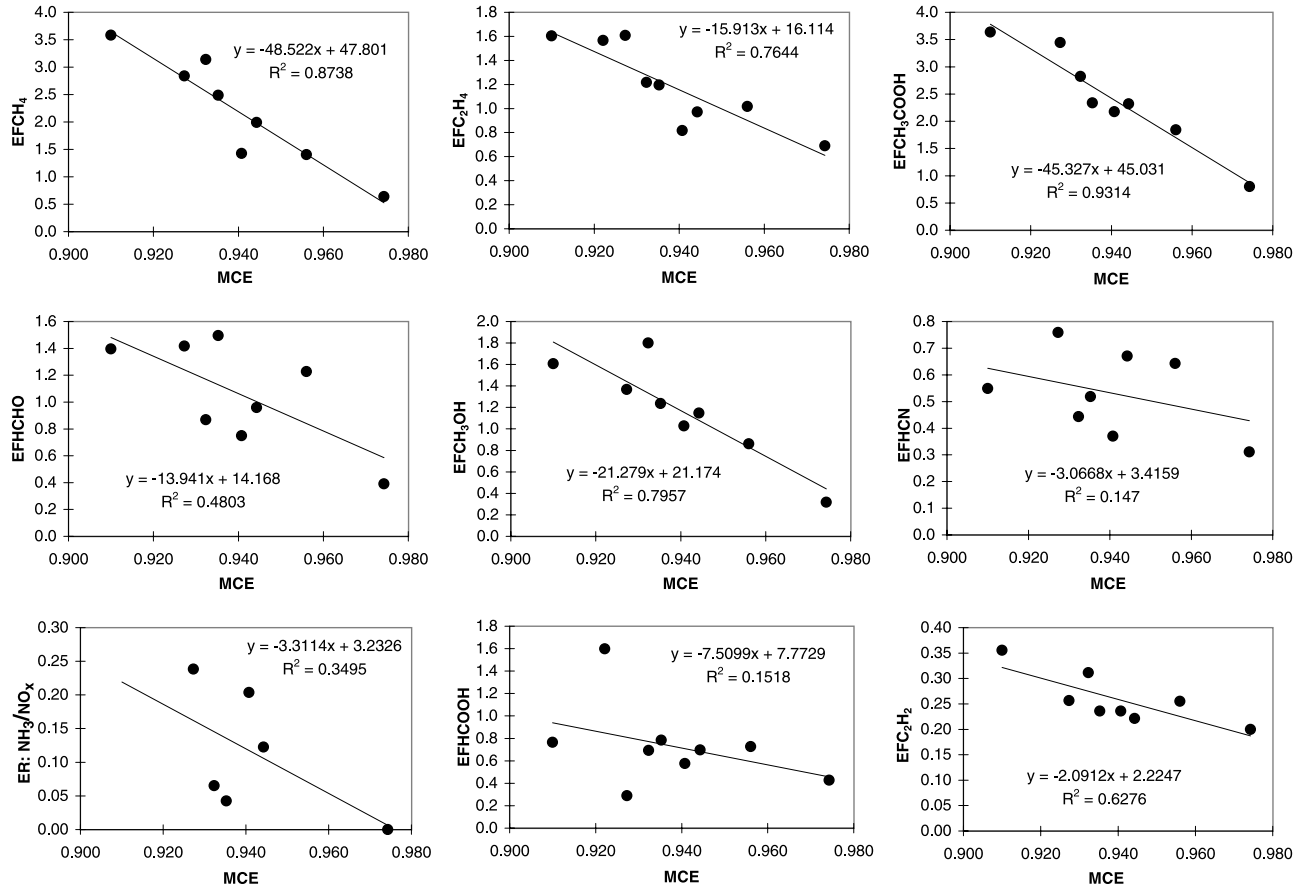

Figure 3. The fire-average initial emission ratios are used to derive fire-average initial emission factors (EF, g/kg dry fuel) and fire-average MCE as discussed in section 3.2.4. For the smoldering compounds measured in this study (except CO) we plot the initial EF for each fire versus fire-average MCE. The figure shows a range of fire-average EF and the dependence of EF on the different relative amount of flaming and smoldering that can occur during different fires. The plots are in order of molar abundance (from upper left). $EFNH_3$ ranged from zero to 0.4 g/kg, but we plot the emission ratio NH_3/NO_x instead to normalize the effects of varying fuel nitrogen content and to facilitate the discussion in section 3.2.6.

total fuel consumption during RSC, EF_{AB} the emission factor measured in-situ from an airborne platform, and F_{AB} the fraction of total fuel consumed for which the emissions are entrained in a convective plume. From equation (1) we expect a very small correction for pure grass fires since F_{RSC} is very small. However, a larger correction could occur in wooded savannas where large diameter, downed logs may be present (especially further from villages where such logs are harder to utilize as fuel). Ground-based fuel measurements for the planned fire in the miombo (UW Flight 1826) suggest that up to 10% of the total fuel consumption was due to logs that continued smoldering after strong convection from the fire had ceased (J. Pereira et al., personal communication, 2002). In addition, *Bertschi et al.* [2003b] found that the EF for smoldering logs in the miombo were very different from the miombo fire EF in this work. The net result is that if we assume 10% of fuel consumption by RSC (of logs) in equation (1) the emission factors for selected compounds are increased by the following factors: CH_4 (2.5), CH_3OH (1.7), NH_3 (1.4), HCHO (1.4), and CH_3COOH (1.3). The effects on MCE and other species are smaller [*Bertschi et al.*, 2003b].

[25] In summary, the assumption that all carbon emissions are detected causes a slight overestimate of EF as discussed in section 3.2.4. However, RSC probably increases the real EF for smoldering compounds toward the end of the dry season (especially in the wooded savannas as the large diameter fuels dry out). In addition, the tendency for some early dry season fires to have lower MCE [*Hoffa et al.*, 1999] could indicate that they have higher EF for smoldering compounds. Thus, the EF in Table 2 may mostly be conservative estimates. Clearly, more work is needed to quantify the influence of these important, complicating factors.

3.2.6. Comparison of ER and EF to Previous Work and Implications

[26] The emission factors and emission ratios presented here agree well with previous measurements in many cases. However, we also report a significant amount of improved or unique data for important fire emissions. *Andreae and Merlet* [2001, hereafter AM2001] reviewed previous emissions measurements for savanna fires. Therefore, we will

often compare our measurements to the values they reported. Fires can exhibit high variability so the comparisons should not be over interpreted. In addition, AM2001 often calculated EF assuming 45% carbon in the fuel, which would reduce the EF by 10% compared to ours. Thus, we deem agreement within 10% as excellent. Our average EF and ER for savanna fires are in Table 2.

[27] CO_2 and CO are the two most abundant emissions from biomass fires (excluding water). Our study-average EF for both these compounds are above the average values given by AM2001, but within their range. The ratio between CO_2 and CO, the combustion characteristics of fires, and equations for predicting EF for other trace gases are all related to the MCE. AM2001 reported an average MCE of 0.940 ($\Delta CO/\Delta CO_2 = 0.063$) for previous fire measurements in global tropical savannas. Their data set included mostly South African fires; 60% of the fires in our data set were also in South Africa, and we obtain a study-average MCE value of 0.938 ($\Delta CO/\Delta CO_2 = 0.066$). Despite this good agreement with AM2001, a different average MCE for African savanna fires can be computed that is based on our measurements for humid savanna fires. If we assume that the humid savanna region is 80% miombo and 20% dambo, that the miombo areas burn every two years, and the dambos burn annually [*Desanker et al.*, 1997], then the weighted average MCE is 0.952 (Table 2, last column). This ''humid savanna'' MCE value is only a little higher than our study-average MCE and the ''real'' average humid savanna MCE could be reduced by early season fires and RSC as discussed earlier.

[28] The major hydrocarbon emitted from fires is CH_4. *Ward et al.* [1992] developed a model for global methane emissions that predicts the EF of CH_4 ($EFCH_4$) as a function of combustion efficiency (CE, the fraction of burned fuel carbon released as CO_2). Our study-average $EFCH_4$ (2.2 g/kg) lies on their savanna-fire regression line at our estimated study-average CE of 0.927. The slope of our plot of $EFCH_4$ versus MCE is larger than their slope for $EFCH_4$ versus CE, but our slope is decreased if we plot versus CE and it is also based on a smaller range of values for the independent variable. Our average $\Delta CH_4/\Delta CO$ ER is 5.3%, which is lower than the AM2001 ER of 6.1%, but our average $EFCH_4$ (2.2 ± 1.0 g/kg) is very close to the AM2001 value for savanna fires of 2.3 ± 0.9 g/kg. We also measured EF for two C_2 hydrocarbons. The EF for C_2H_2 were not strongly dependent on MCE, in agreement with *Lobert et al.* [1991] who determined that C_2H_2 was produced by both flaming and smoldering combustion. Our EF for C_2H_4 and C_2H_2 are 150% and 90%, respectively, of the AM2001 values, but well within their large range. In deriving ''preferred'' EF values based on previous measurements, AM2001 may have included some data from aged smoke, which would have depleted levels of many reactive initial emissions such as C_2H_4 [e.g., *Blake et al.,* 1996; *Lee et al.*, 1997].

[29] In this work we report the first quantitative measurements of the emissions of oxygenated volatile organic compounds (OVOC) from African savanna fires. Earlier ground based and airborne FTIR studies showed that OVOC are major emissions from temperate and boreal fires [*Griffith et al.*, 1991; *Yokelson et al.*, 1996, 1997, 1999; *Worden et al.*, 1997; *Goode et al.*, 1999, 2000], but no quantitative measurements of OVOC were available for any African fires. *Koppmann et al.* [1997] had reported some ''lower limits'' for selected high molecular-weight, semivolatile oxygenated organic compounds emitted by fires in sugar cane plantations and forests in South Africa. They concluded that these compounds were probably at least as common as ''heavy'' hydrocarbons. *Yokelson et al.* [1999] predicted both the identity and the average EF of the three main OVOC emitted by African savanna fires based on a linear fit of the EF versus MCE for fires in temperate regions. These predictions (in units of g/kg), followed by our study-average value in parentheses, are: HCHO, 1.6 (1.0); CH_3OH, 1.1 (1.2); and acetic acid 2.5 (2.4). The predictions are generally close and our African, fire-average EF lie tightly clustered about regression lines fit to EF versus MCE for fires in aboveground fine fuels from temperate, boreal, and tropical ecosystems [*Yokelson et al.*, 1999; *Goode et al.*, 2000; this work] (see Figure 4). This suggests that these plots are useful globally for predicting OVOC emissions from fires in aboveground fine fuels [*Bertschi et al.*, 2003b]. AM2001 also estimated EFs (in an unspecified manner) for the above oxygenates, which were close to our measurements for methanol, but factors of 2 and 3 lower than our measurements for acetic acid and formaldehyde.

[30] A major goal of our work in S2K was to determine if OVOC are important emissions from African savanna fires. In fact, the sum of the EF for the OVOC we measured is 5.30 g/kg, which is considerably larger than the sum of the EF for the hydrocarbons we detected (including methane) of 3.26 g/kg. The influence of tropical fire emissions has been studied with numerous atmospheric photochemical models [*Chatfield and Delaney*, 1990; *Fishman et al.*, 1991; *Richardson et al.*, 1991; *Keller et al.*, 1991; *Crutzen and Carmichael*, 1993; *Chatfield et al.*, 1996; *Thompson et al.*, 1996; *Jacob et al.*, 1996; *Koppmann et al.*, 1997; *Lelieveld et al.*, 1997; *Olson et al.*, 1997; *Mauzerall et al.*, 1998; *Lee et al.*, 1998], but none have included OVOC as initial emissions. However, *Mason et al.* [2001] showed that the OVOC we quantified in this work have a large effect on the production of ozone, HO_x, hydrogen peroxide, and the distribution of nitrogen reservoir species in smoke plume models. Their results and the measurements reported here show that OVOC should be included in future modeling studies of African fire emissions.

[31] We report several interesting observations regarding the emission of nitrogen-containing compounds from African savanna fires. HCN has significance both as a possible biomass-burning tracer [*Cicerone and Zellner*, 1983; *Rinsland et al.*, 2000; *Li et al.*, 2000], and as potential interference in measurements of NO_y [*Fahey et al.*, 1985; *Kliner et al.*, 1997]. Both *Lobert et al.* [1991] and *Yokelson et al.* [1997] reported that HCN was emitted in highly variable amounts by smoldering combustion of various types of biomass ($\Delta HCN/\Delta CO$ from ~0–5%). AM2001 recommended an EFHCN of 0.025–0.031 g/kg for savanna fires based on the only previous savanna-fire field measurements (in Australia) [*Hurst et al.*, 1994a, 1994b], which were near the low end of previous biomass-burning measurements. Our EFHCN (0.53 ± 0.14 g/kg) is ~20 times higher. Despite the variability noted above, in our savanna fire data EFHCN is not strongly dependent on MCE, and the average

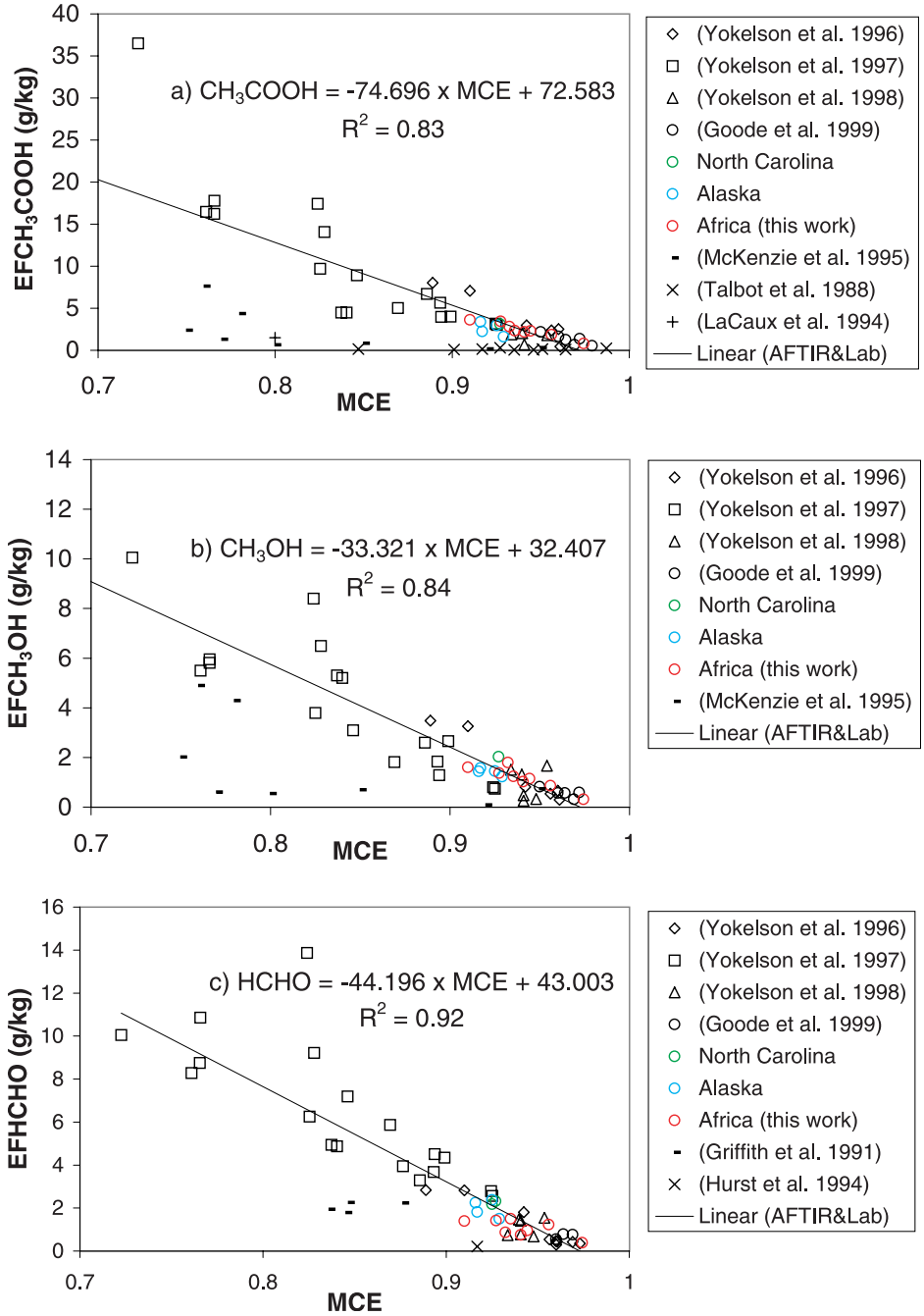

Figure 4. Emission factors plotted against MCE for (a) acetic acid, (b) methanol, and (c) formaldehyde; the major oxygenated organic compounds emitted by fires. The linear regression lines were fit to all the airborne FTIR results (colored symbols) from southern Africa [this work], Alaska [*Goode et al.*, 2000], and North Carolina [*Yokelson et al.*, 1999], and the open-path FTIR laboratory results (black, closed, unfilled symbols) for a wide variety of aboveground fine fuels. Some results from other techniques are also shown for comparison. The FTIR-based field and laboratory data are both close to the regression line for each compound. The regression equations (shown) can be used to estimate the initial emissions of these important compounds as discussed in section 3.2.6.

EF is a reasonable value for all our savanna fires. In addition, *Bertschi et al.* [2003a] saw no evidence of HCN emissions from the production and use of domestic biomass fuels. Column HCN can be monitored by automated, ground-based [*Rinsland et al.*, 2000] or space-based instrumentation [*Li et al.*, 2000]. These factors suggest that HCN may have value as a tracer for savanna fire emissions. However, the effect of seasonal variation in fuel moisture and nitrogen content on HCN emissions should be investigated. *Kliner et al.* [1997] made a detailed study of the influence of pressure, ozone, water, catalyst condition, and choice of reducing agent on HCN conversion in NO_y

instruments. Since HCN conversion was 100% under some conditions, some previous NO_y measurements in air impacted by biomass burning may be in error.

[32] Our study-average emission factor for NO_x (as NO) of 3.37 ± 0.64 g/kg is in reasonable agreement with the AM2001 recommendation of 3.9 ± 2.4 g/kg. There was a surprisingly large ER for $\Delta NO_x/\Delta CO$ for the dambo fire sampled on 5 September (UW Flight 1831), which can be deduced from Table 2. The ER was ~8%, which is closer to the values usually found for fossil fuel combustion (~10%) than for extratropical biomass burning (1–4%). This high ratio resulted from the very high flaming/smoldering ratio for this fire, as seen in the very low $\Delta CO/\Delta CO_2$ ER (2.64% or MCE = 0.974); the $\Delta NO_x/\Delta CO_2$ ER for this fire (0.2%) is within the usual range for biomass burning (AM2001).

[33] We measured variable ammonia emissions from savanna fires. The $\Delta NH_3/\Delta CO$ ER was very high (up to 4.5%) near the beginning and end of the miombo fire (UW Flight 1826, Table 1) when smoldering dominated. In contrast, there were never any detectable ammonia spectral signals during the dambo fire (UW Flight 1831, Table 1). Also, the $\Delta NH_3/\Delta CO$ ER measured with our artifact-free, open-path FTIR system at much higher smoke concentrations produced by fires in dambo grasses in both Zambia and 10 recent laboratory burns (T. J. Christian et al., manuscript in preparation, 2003) confirm that NH_3 was very likely below our detection limits in our airborne samples of the dambo fire. These low NH_3 emissions could be partly due to the high flaming/smoldering ratio or the low fuel nitrogen content since we measured an average N content for two samples of dambo grass (collected in the late dry season) of 0.22%, or about 1/5 of the average value for biomass. (The miombo litter samples averaged 1.2% N.) We conclude that NH_3 emissions from dambo fires are very small late in the dry season. (They could be higher earlier in the dry season when the grass has higher N content and fuel moisture.) Because of fuel nitrogen variability, *Goode et al.* [2000] plotted the ER $\Delta NH_3/\Delta NO_x$ versus MCE for fires mostly in temperate and boreal fuels. Our value of "zero" for this ER at the high MCE of the dambo fire is reasonably consistent with their model, but the $\Delta NH_3/\Delta NO_x$ ER for our other savanna fires at lower MCEs are less than half of what was measured with similar instrumentation for extratropical fires at similar MCEs (Figure 3) [see also *Goode et al.*, 2000, Figure 4]. If we correct our $\Delta NH_3/\Delta NO_x$ ER for the impact of residual smoldering combustion (see section 3.2.5) it raises the ER for our Miombo fire by 42%. Nevertheless, it seems that NH_3 emissions from late-season savanna fires are indeed lower, on the average, than from most extratropical fires. Finally, our study-average $EFNH_3$ for savanna fires (0.28 ± 0.14 g/kg) is ~10 times larger than the one previous NH_3 measurement for African savanna fires [*Delmas et al.*, 1995], but, it is 2–5 times lower than the values recommended by AM2001 based on the work of *Hurst et al.* [1994a, 1994b] in Australia. Thus, any uncertainty in our NH_3 measurements is small compared to the differences between our values and those reported previously.

[34] We conclude this section by coupling data in Table 2 with that of *Cofer et al.* [1996] for H_2, *Kuhlbusch et al.* [1991] for N_2, and *Sinha et al.* [2003a] for SO_2 to make a reasonably complete list of the top 15 trace gases directly emitted by African savanna fires (excluding water). The gases are listed next in the format: (rank in order of moles produced), chemical formula, and ER to CO_2 (ppb/ppm). (1) CO_2 1000, (2) CO 66.4, (3) H_2 12.6, (4) CH_4 3.53, (5) NO_x 3.10, (6) N_2 2.87 (7) C_2H_4 1.14, (8) CH_3COOH 1.06, (9) HCHO 0.97, (10) CH_3OH 0.96, (11) SO_2 0.85, (12) HCN 0.57, (13) NH_3 0.47, (14) HCOOH 0.39, (15) C_2H_2 0.29. This paper reports the first quantitative data obtained in Africa for 6 of the 15 most abundant trace gases produced by savanna fires.

3.3. Observations of Post Emission Smoke Processing

[35] Eleven of the fifteen most abundant trace gases emitted by savanna fires (listed above) are too reactive to become well mixed in the global troposphere. Photochemistry and other processes rapidly consume many of the initial emissions and produce new species. Determining the influence of biomass burning on local to global scales requires good emissions estimates, but also detailed understanding of the complex, postemission transformations, which can occur in smoke plumes that are very different from the "normal" atmosphere. We describe some significant postemission changes in the chemical composition of smoke due to photochemical or cloud processing. These observations also highlight the importance of using only nascent smoke samples for calculating initial emissions from biomass fires.

3.3.1. Rapid Photochemical Formation of Ozone and Acetic Acid

[36] Measuring the photochemical changes in plumes downwind of fires is complicated by the fact that the mixing ratios in a parcel of smoke change due to photochemistry, heterogeneous processes, and mixing. CO has a lifetime of about one month in the tropical troposphere and so, up to several days downwind from a fire, the CO mixing ratios can indicate the plume location and the rate of mixing. Photochemical transformations in a smoke parcel change the ratio of a compounds excess mixing ratio to that of CO. In particular, photochemistry involving NO_x, CO, and organic compounds produces O_3 and other products and therefore, the $\Delta O_3/\Delta CO$ ratio has often been used as an indicator of the degree of photochemical aging for smoke/haze samples [*Andreae et al.*, 1988, 1994; *Goode et al.*, 2000] and in modeling studies [e.g., *Chatfield and Delaney*, 1990; *Jacob et al.*, 1992, 1996; *Mauzerall et al.*, 1998].

[37] Our AFTIR spectra of minutes-old, African smoke show large, negative, excess ozone mixing ratios (Table 1), as found also for a fire in the Pacific Northwest by *Stith et al.* [1981]. This is due to destruction of O_3 by NO, HO_2, and particles. Multiplying these large, negative, excess O_3 values by −1 yields a lower limit for the ozone mixing ratios in the entrained background air, which, in Africa, were as high as 100 ppb (Table 1, Flights 1816, 1819, 1826, 1831, 1834). (These low-altitude results suggest that vast regions of southern Africa can have dry-season, surface ozone mixing ratios above 50 ppbv, which is the US EPA, 8-hour average, permissible exposure limit.)

[38] We sampled biomass-burning plumes both at their source and up to ~30 km downwind on three occasions during S2K: Flight 1825 (Beira Fire, 31 August), Flight 1826 (Miombo Fire, 1 September), and Flight 1834 (Timbavati Fire, 7 September). In all cases we observed an "O_3 hole" in nascent smoke followed by rapid production of

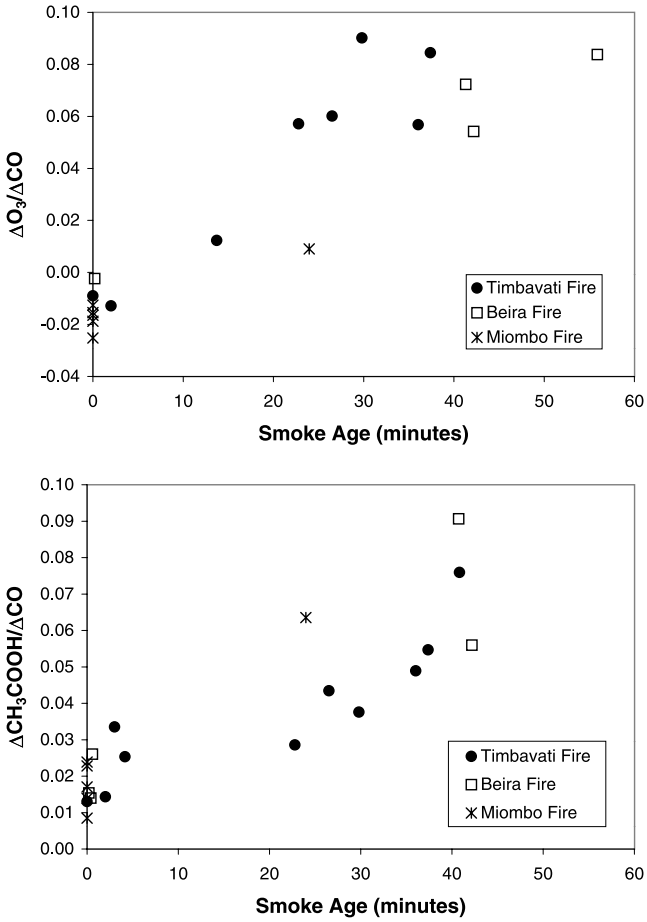

Figure 5. The rapid change in smoke composition due to photochemical processing is evident in the increasing ratios of excess O_3 and CH_3COOH (acetic acid) to excess CO as a function of smoke age. Excess O_3 and CH_3COOH rise to levels comparable to excess CH_4 in less than an hour. The average transport speed for the smoke (in m/s) was Timbavati 11.3, Beira 7.9, and Miombo 5.7.

both O_3 and acetic acid. In Figure 5 we illustrate the downwind changes in O_3 and acetic acid for these fires by plotting $\Delta O_3/\Delta CO$ and $\Delta CH_3COOH/\Delta CO$ versus smoke age. $\Delta O_3/\Delta CO$ increased to as much as 9% in less than 1 hour, which can be compared to the value of 22% we measured in biomass burning haze 2–4 days old off Namibia (UW Flight 1837) and 20–88% measured in biomass burning haze about 10 days transport time from Africa by *Andreae et al.* [1994]. $\Delta CH_3COOH/\Delta CO$ also rose to as much as 9% less than 1 hour downwind, which was more than 5 times the initial emission ratio (Beira Fire). Our measurements of the changing ratios in the downwind plumes could partly reflect changes in the source ratio since these were not Lagrangian experiments. However, on Flight 1834, we remeasured the source ratios ~1 h after our first source samples and the source variation was much smaller than the downwind variation. On Flight 1826 the downwind plume was intersected by younger smoke from another fire. Thus, for this fire only, the smoke age is not clearly defined. One possible explanation of the downwind data for this fire is that the injection of fresh emissions destroyed some O_3, but spurred CH_3COOH production.

[39] The initial emissions of acetic acid from savanna fires are much higher than previously thought [*Talbot et al.*, 1996] and additional, rapid secondary production occurs (as was also observed in Alaska [*Goode et al.*, 2000]). For example, on a mass basis, acetic acid is the most abundant organic initial emission from savanna fires and its ratio to CO more than triples after emission. The main sink of acetic acid is thought to be reaction with OH, but the products are unknown. *Jacob et al.* [1996] found that their photochemical model was sensitive to different assumptions about these products. Given the high levels of acetic acid that we observe, determining the products of its reaction with OH is of considerable importance. Finally, we did not see consistent, strong evidence of downwind production of formic acid in Africa as was observed in Alaska [*Goode et al.*, 2000].

[40] In summary, major changes in the chemistry of savanna-fire smoke during the first hour of aging include: (1) excess ozone and excess acetic acid rise to levels comparable to, or greater than, excess methane, and (2) NO_x is rapidly converted to reservoir species [*Mason et al.*, 2001]. *Hobbs et al.* [2003] compare the rates of production for O_3 and CH_3COOH reported here to those measured in other biomass-burning plumes by *Goode et al.* [2000] and *Hobbs et al.* [1996]. The changes in hydrocarbons and particle concentrations with smoke age are also discussed [*Hobbs et al.*, 2003]. *Jost et al.* [2003] describe photochemistry observed in a Namibian biomass-burning plume during S2K.

3.3.2. Cloud-Induced Changes in the Chemical Composition of Smoke

[41] During the planned fire at Madikwe Game Reserve on 18 August, a large cumulus cloud capped the vertical column of smoke ~3 km above the flame front (see photo at http://www.umt.edu/chemistry/faculty/yokelson/galleries/s2k/jpg_madikwe.htm). This provided an opportunity to compare a sample of nascent smoke below the cloud (Table 1, UW Flight 1816, altitude 1945 m) with two samples of increasingly cloud-processed smoke (altitude 3866 and 4166 m, respectively).

[42] Figure 6 shows the changes in $\Delta X/\Delta CO$ with increased cloud-processing for 6 gases (CO is used as a tracer). A dramatic "disappearance" of CH_3OH and NH_3 occurred in the cloud-processed smoke. The NO_2 and acetic acid ratios to CO also decreased markedly. In addition, the UW SO_2 analyzer indicated that SO_2 was removed from the plume at a rate similar to methanol. In contrast, $\Delta NO/\Delta CO$ and $\Delta HCHO/\Delta CO$ increased significantly and $\Delta CO/\Delta CO_2$ increased slightly (Table 1). The HCHO increase could be due to enhanced photochemistry in the cloud margins [*Madronich*, 1987] or heterogeneous conversion of CH_3OH to HCHO [*Singh et al.*, 2000]. The large decrease in $\Delta NO_2/\Delta NO$ could be due to enhanced photolysis of NO_2 or HONO (formed from NO_2 on particle surfaces). Other possibilities are discussed by *Ravishankara and Longfellow* [1999]. CH_3OH, NH_3, CH_3COOH, and SO_2 probably decreased because of their solubility. However, the relative rates of these decreases are not proportional to the Henry's Law constants for the gases [*Betterton*, 1992], which suggests that not all the gases reached equilibrium with the cloud water; possibly due to reactions of the dissolved gases in solution. If such reactions

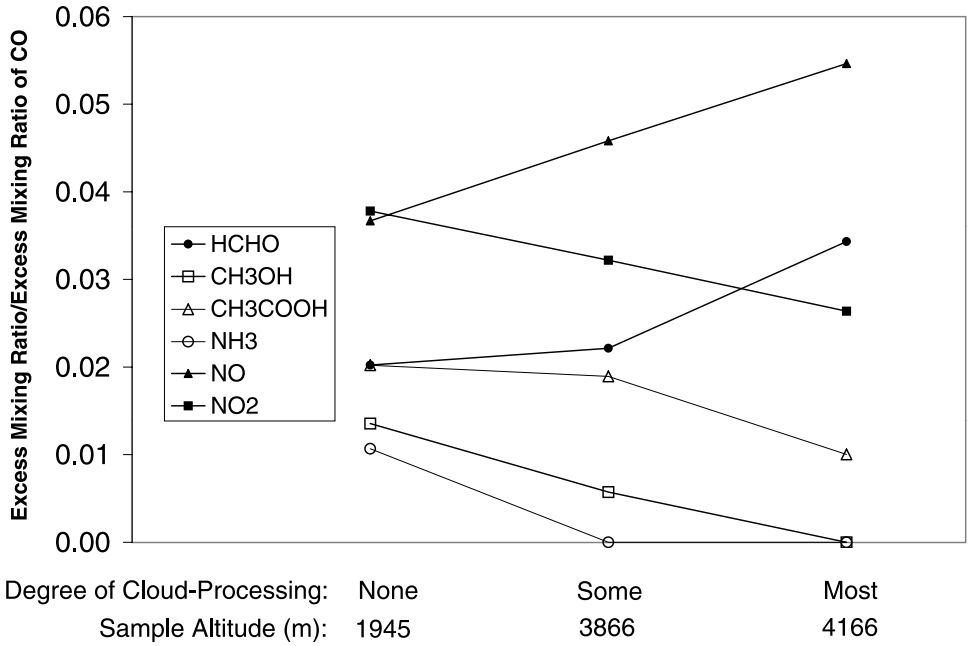

Figure 6. Excess mixing ratios of various species divided by the simultaneously measured excess mixing ratio of CO as a function of the degree of cloud processing. Cloud effects on the gases are decoupled from the effects of dilution by comparison to CO, which is an insoluble tracer. The observations are discussed in section 3.3.2.

occurred, the gases would not be released in their original concentrations if the cloud droplets evaporated [e.g., *Easter and Hobbs*, 1974]. Based on the size of the cloud and the wind speed, the cloud-processing effects probably occurred within a few minutes. The single sample obtained from the Lebombo Fire (Table 1, UW Flight 1825, altitude 3874 m) has characteristics consistent with moderate cloud processing since it showed lower than "normal" $\Delta CH_3OH/\Delta CO$, $\Delta CH_3COOH/\Delta CO$, and $\Delta NH_3/\Delta CO$, and higher than "normal" $\Delta HCHO/\Delta CO$ and $\Delta NO/\Delta NO_2$. Although clouds were not observed near this fire, it is possible that a capping cumulus cloud processed the smoke before we arrived since the smoke plume dynamics were similar to those observed during the Madikwe fire.

[43] The above observations justify omitting cloud-processed samples from the calculation of initial emission factors for many species. They also show that the transport of smoke in convective clouds is likely accompanied by fast, significant changes in smoke chemistry. The large influence of OVOC on smoke chemistry demonstrated by *Mason et al.* [2001] will be strongly altered if the concentrations of OVOC are changed by cloud-processing. The delay between emission and cloud-processing is important since photochemical processing of OVOC leads to high levels of H_2O_2 in hours-old smoke [*Mason et al.*, 2001]. On a broader scale, clouds (which cover 50% of the Earth on the average) could have similar effects on biogenic emissions, which include high levels of soluble oxygenates such as methanol [*Konig et al.*, 1995; *Kirstine et al.*, 1998]. In general, OVOC that are released or produced in the boundary layer and transported vertically by deep convection have a large influence on the HO_x budget of the upper troposphere [*Singh et al.*, 1995], but this influence may depend on cloud processes that are poorly understood.

[44] It is intriguing to estimate the amount of gases "scavenged" from the smoke by the capping cloud on UW Flight 1816. For example, based on the $\Delta CH_3OH/\Delta CO$ ratio below the cloud, and ΔCO in the most heavily cloud processed sample, a simple calculation suggests that 25 $\mu g/m^3$ of CH_3OH alone were removed from the smoke by the cloud. In contrast, *Decesari et al.* [2000] reported an average total dissolved matter content of 28 $\mu g/m^3$ (inorganic + organic) in polluted fog droplets in the Po River Valley. Comparison of these numbers suggests that clouds impacted by smoke can be extremely "dirty" and have high potential for intense multiphase chemistry and the generation of enriched new particles in the cloud detrainment zone [*Ravishankara and Longfellow*, 1999].

4. Conclusions

[45] We deployed an FTIR coupled to a multipass cell on the University of Washington's Convair-580 research aircraft to measure stable and reactive trace gases in southern Africa during the middle to late dry season (August–September 2000). This is a region and season of extensive biomass burning, which produced well-mixed haze layers that extended to 3.5 km in altitude south of most of the fires, and up to ~6 km in the humid savanna region where most of the burning occurs. We observed high CO, O_3, and water vapor in the haze layers. At the top of the haze layers there was usually a sharp transition to the much cleaner and drier free troposphere. Cumulus convection in nonprecipitating clouds played a potentially significant role in mixing these two different layers. We measured the vertical profiles of CO and other gases above instrumented ground sites and below the NASA ER-2 and overpasses by the TERRA satellite.

[46] The use of FTIR gave us the capability to measure most of the major trace gases emitted by 10 savanna fires that were representative of the fires that feed the haze layers (including two fires in the important humid savanna region). Measurements made in nascent smoke, throughout the course of the fires, and during peak, regional smoke levels were used to calculate initial emission factors. We report savanna fire emission factors for (in order of molar abundance) CO_2, CO, CH_4, NO_x (as NO), C_2H_4, CH_3COOH, HCHO, CH_3OH, HCN, NH_3, HCOOH, and C_2H_2. The initial emission factors for some smoldering compounds could be higher early in the dry season [*Hoffa et al.*, 1999] or where large-diameter fuels contribute to residual smoldering combustion [*Bertschi et al.*, 2003b]. These are the first quantitative measurements in Africa for 6 of the 15 most abundant trace gases emitted by savanna fires. Oxygenated organic compounds (which react photochemically to produce HO_x) accounted for 70% of the nonmethane organic compounds emitted by savanna fires. Since savanna fires are a major global source of trace gases, this has implications for the tropospheric HO_x budget [*Mason et al.*, 2001]. We measured a large emission factor for HCN from savanna fires, but observed no HCN emissions from the production and use of domestic biofuels in a separate study [*Bertschi et al.*, 2003a]. Thus, HCN may be useful as a tracer for savanna fires. The large HCN emissions may also mean that some NO_y measurements made in air impacted by fires are in error [*Kliner et al.*, 1997]. NH_3 emissions were found to be much higher than previously measured for African savanna fires, but lower than measured for Australian savanna fires [*Hurst et al.*, 1994a, 1994b].

[47] We observed significant, postemission production of acetic acid and ozone in smoke samples of measured ages from two fires. These are the first precise observations of photochemical rates in African smoke [*Hobbs et al.*, 2003]. $\Delta CH_3COOH/\Delta CO$ and $\Delta O_3/\Delta CO$ rose to levels as large as 9% ($>\Delta CH_4/\Delta CO$) in <1 h. Acetic acid was a major, initial organic emission and the major excess organic compound in ~1 hour-old smoke. Thus, the products of the reaction of acetic acid with OH need to be determined. We also observed fast, cloud-induced changes in smoke chemistry. Methanol, CH_3COOH, NO_2, and NH_3 were significantly reduced by exposure to clouds, but not at relative rates proportional to their Henry's Law constants. Cloud processing significantly increased HCHO and NO.

[48] Photochemical, cloud, and other processes rapidly and dramatically change smoke long before it becomes even locally mixed. Thus, many primary pollutants would be measured incorrectly in smoke more than a few minutes old. However, airborne measurements in nascent smoke compare well to laboratory smoke measurements (see Figure 4). The rapid evolution of smoke by cloud-processing and photochemistry occurs in an environment that is very different from ''ambient'' air. The timing between photochemical and cloud processing will also strongly affect the outcome. The postemission transformations critically influence the regional-global impact of biomass burning.

[49] **Acknowledgments.** This research was supported by funds provided by the National Science Foundation under grants ATM-9900494 and ATM-9901624, the Interagency Joint Fire Science Program, the Rocky Mountain Research Station, Forest Service, U.S. Department of Agriculture (INT-97082-RJVA and RMRS-99508-RJVA) and NASA grants NAGS-9022 and NAGS-7675. The authors thank Michael King, Bob Swap, Harold Annegarn, and Tim Suttles for their major role in SAFARI 2000 activities and NASA and the C-131 crew for logistical support. The UM personnel thank the UW Convair-580 crew and pilots for their support.

References

Andreae, M. O., Emissions of trace gases and aerosols from southern African savanna fires, in *Fire in Southern African Savannas: Ecological and Atmospheric Perspectives*, edited by B. W. van Wilgen, M. O. Andreae, J. G. Goldammer, and J. A. Lindesay, pp. 161–183, Witwatersrand Univ. Press, Johannesburg, South Africa, 1997.

Andreae, M. O., and P. Merlet, Emissions of trace gases and aerosols from biomass burning, *Global Biogeochem. Cycles*, *15*, 955–966, 2001.

Andreae, M. O., et al., Biomass-burning emissions and associated haze layers over Amazonia, *J. Geophys. Res.*, *93*, 1509–1527, 1988.

Andreae, M. O., B. E. Anderson, D. R. Blake, J. D. Bradshaw, J. E. Collins, G. L. Gregory, G. W. Sachse, and M. C. Shipham, Influence of plumes from biomass burning on atmospheric chemistry over the equatorial and tropical South Atlantic during CITE 3, *J. Geophys. Res.*, *99*, 12,793–12,808, 1994.

Andreae, M. O., E. Atlas, H. Cachier, W. R. Cofer III, G. W. Harris, G. Helas, R. Koppmann, J.-P. Lacaux, and D. E. Ward, Trace gas and aerosol emissions from savanna fires, in *Biomass Burning and Global Change*, edited by J. S. Levine, pp. 278–295, MIT Press, Cambridge, Mass., 1996.

Bertschi, I. T., R. J. Yokelson, D. E. Ward, T. J. Christian, and W. M. Hao, Trace gas emissions from the production and use of domestic biofuels in Zambia measured by open-path Fourier transform infrared spectroscopy, *J. Geophys. Res.*, *108*, doi:10.1029/2002JD002158, in press, 2003a.

Bertschi, I., R. J. Yokelson, D. E. Ward, J. G. Goode, R. Babbitt, R. A. Susott, and W. M. Hao, The trace gas and particle emissions from fires in large-diameter and belowground biomass fuels, *J. Geophys. Res.*, *108*, doi:10.1029/2002JD002100, in press, 2003b.

Betterton, E. A., Henry's law constants of soluble and moderately soluble organic gases: Effects on aqueous phase chemistry, in *Gaseous Pollutants: Characterization and Cycling*, edited by J. O. Nriagu, pp. 1–50, John Wiley, New York, 1992.

Blake, N. J., D. R. Blake, B. C. Sive, T. Y. Chen, F. S. Rowland, J. E. Collins, G. W. Sachse, and B. E. Anderson, Biomass burning emissions and vertical distribution of atmospheric methyl halides and other reduced carbon gases in the South Atlantic region, *J. Geophys. Res.*, *101*, 24,151–24,164, 1996.

Browell, E. V., et al., Ozone and aerosol distributions and air mass characteristics over the South Atlantic basin during the burning season, *J. Geophys. Res.*, *101*, 24,043–24,068, 1996.

Cahoon, D. R., Jr., B. J. Stocks, J. S. Levine, W. R. Cofer III, and K. P. O'Neill, Seasonal distribution of African savanna fires, *Nature*, *359*, 812–815, 1992.

Chatfield, R. B., and A. C. Delaney, Convection links biomass burning to increased tropical ozone: However, models will tend to overpredict O_3, *J. Geophys. Res.*, *95*, 18,473–18,488, 1990.

Chatfield, R. B., J. A. Vastano, H. B. Singh, and G. W. Sachse, A general model of how fire emissions and chemistry produce African/oceanic plumes (O_3, CO, PAN, smoke) in TRACE A, *J. Geophys. Res.*, *101*, 24,279–24,306, 1996.

Cicerone, R. J., and R. Zellner, The atmospheric chemistry of hydrogen cyanide (HCN), *J. Geophys. Res.*, *88*, 10,689–10,696, 1983.

Cofer, W. R., III, J. S. Levine, E. L. Winstead, D. R. Cahoon, D. I. Sebacher, J. P. Pinto, and B. J. Stocks, Source compositions of trace gases released during African savanna fires, *J. Geophys. Res.*, *101*, 23,597–23,602, 1996.

Crutzen, P. J., and M. O. Andreae, Biomass burning in the tropics: Impact on atmospheric chemistry and biogeochemical cycles, *Science*, *250*, 1669–1678, 1990.

Crutzen, P. J., and G. R. Carmichael, Modeling the influence of fires on atmospheric chemistry, in *Fire in the Environment: The Ecological, Atmospheric, and Climatic Importance of Vegetation Fires*, edited by P. J. Crutzen and J. G. Goldammer, pp. 89–105, John Wiley, New York, 1993.

Decesari, S., M. C. Facchini, E. Matta, and S. Fuzzi, Organic and inorganic solutes in fog droplets: A full characterization approach, paper presented at 13th International Conference on Clouds and Precipitation, Reno, NV, USA, 14–18 August, 2000.

Delmas, R., J. P. Lacaux, J. C. Menaut, L. Abbadie, X. Le Roux, G. Helas, and J. Lobert, Nitrogen compound emissions from biomass burning in tropical African savanna FOS/DECAFE 1991 experiment (Lamto, Ivory Coast), *J. Atmos. Chem.*, *22*, 175–193, 1995.

Desanker, P. V., , P. G. H. Frost, C. O. Justice, and R. J. Scholes (Eds.), *The Miombo Network: Framework for a Terrestrial Transect Study of Land-*

Use and Land-Cover Change in the Miombo Ecosystems of Central Africa, Conclusions of the Miombo Network Workshop Zomba, Malawi, December 1995, *IGBP Rep. 41*, 109 pp., IGBP, Stockholm, 1997.

Easter, R. C., and P. V. Hobbs, The formation of sulfates and the enhancement of cloud condensation nuclei in clouds, *J. Atmos. Sci.*, *35*, 1586–1594, 1974.

Eck, T. F., et al., Variability of biomass burning aerosol optical characteristics in southern Africa during the SAFARI 2000 dry season campaign and a comparison of single scattering albedo estimates from radiometric measurements, *J. Geophys. Res.*, *108*, doi:10.1029/2002JD002321, in press, 2003.

Fahey, D. W., C. S. Eubank, G. Hubler, and F. C. Fehsenfeld, Evaluation of a catalytic reduction technique for the measurement of total reactive odd-nitrogen NO_y in the atmosphere, *J. Atmos. Chem.*, *3*, 435–468, 1985.

Fishman, J., K. Fakhruzzaman, B. Cros, and D. Nganga, Identification of widespread pollution in the Southern Hemisphere deduced from satellite analyses, *Science*, *252*, 1693–1696, 1991.

Fishman, J., J. H. Hoell Jr., R. D. Bendura, R. J. McNeal, and V. W. J. H. Kirchoff, NASA GTE TRACE A Experiment (September–October 1992): Overview, *J. Geophys. Res.*, *101*, 23,865–23,880, 1996.

Goode, J. G., R. J. Yokelson, R. A. Susott, and D. E. Ward, Trace gas emissions from laboratory biomass fires measured by open-path Fourier transform infrared spectroscopy: Fires in grass and surface fuels, *J. Geophys. Res.*, *104*, 21,237–21,245, 1999.

Goode, J. G., R. J. Yokelson, D. E. Ward, R. A. Susott, R. E. Babbitt, M. A. Davies, and W. M. Hao, Measurements of excess O_3, CO_2, CO, CH_4, C_2H_4, C_2H_2, HCN, NO, NH_3, HCOOH, CH_3COOH, HCHO, and CH_3OH in 1997 Alaskan biomass burning plumes by airborne Fourier transform infrared spectroscopy (AFTIR), *J. Geophys. Res.*, *105*, 22,147–22,166, 2000.

Griffith, D. W. T., Synthetic calibration and quantitative analysis of gas-phase FTIR spectra, *Appl. Spectrosc.*, *50*, 59–70, 1996.

Griffith, D. W. T., W. G. Mankin, M. T. Coffey, D. E. Ward, and A. Riebau, FTIR remote sensing of biomass burning emissions of CO_2, CO, CH_4, CH_2O, NO, NO_2, NH_3 and N_2O, in *Global Biomass Burning: Atmospheric, Climatic, and Biospheric Implications*, edited by J. S. Levine, pp. 230–239, MIT Press, Cambridge, Mass., 1991.

Hao, W. M., D. E. Ward, G. Olbu, and S. P. Baker, Emissions of CO_2, CO, and hydrocarbons from fires in diverse African savanna ecosystems, *J. Geophys. Res.*, *101*, 23,577–23,584, 1996.

Hobbs, P. V., Clean air slots amid dense atmospheric pollution in southern Africa, *J. Geophys. Res.*, *108*, doi:10.1029/2002JD002156, in press, 2003.

Hobbs, P. V., J. S. Reid, J. A. Herring, J. D. Nance, R. E. Weiss, J. L. Ross, D. A. Hegg, R. D. Ottmar, and C. Liousse, Particle and trace-gas measurements in the smoke from prescribed burns of forest products in the Pacific Northwest, in *Biomass Burning and Global Change*, edited by J. S. Levine, pp. 697–715, MIT Press, Cambridge, Mass., 1996.

Hobbs, P. V., P. Sinha, R. J. Yokelson, T. J. Christian, D. R. Blake, S. Gao, T. W. Kirchstetter, T. Novakov, and P. Pilewskie, Evolution of particle and gas emissions from a savanna fire in South Africa, *J. Geophys. Res.*, *J. Geophys. Res.*, *108*, doi:10.1029/2002JD002352, in press, 2003.

Hoffa, E. A., D. E. Ward, W. M. Hao, R. A. Susott, and R. H. Wakimoto, Seasonality of carbon emissions from biomass burning in a Zambian savanna, *J. Geophys. Res.*, *104*, 13,841–13,853, 1999.

Holzinger, R., C. Warneke, A. Hansel, A. Jordan, W. Lindinger, D. H. Scharffe, G. Schade, and P. J. Crutzen, Biomass burning as a source of formaldehyde, acetaldehyde, methanol, acetone, acetonitrile, and hydrogen cyanide, *Geophys. Res. Lett.*, *26*, 1161–1164, 1999.

Hurst, D. F., D. W. T. Griffith, and G. D. Cook, Trace gas emissions from biomass burning in tropical Australian savannas, *J. Geophys. Res.*, *99*, 16,441–16,456, 1994a.

Hurst, D. F., D. W. T. Griffith, J. N. Carras, D. J. Williams, and P. J. Fraser, Measurements of trace gases emitted by Australian savanna fires during the 1990 dry season, *J. Atmos. Chem.*, *18*, 33–56, 1994b.

Jacob, D. J., et al., Summertime photochemistry of the troposphere at high northern latitudes, *J. Geophys. Res.*, *97*, 16,421–16,431, 1992.

Jacob, D. J., et al., Origin of ozone and NO_x in the tropical troposphere: A photochemical analysis of aircraft observations over the South Atlantic basin, *J. Geophys. Res.*, *101*, 24,235–24,250, 1996.

Jost, C., J. Trentmann, D. Sprung, M. O. Andreae, J. B. McQuaid, and H. Barjat, Trace gas chemistry in a young biomass burning plume over Namibia: Observations and model simulations, *J. Geophys. Res.*, *108*, doi:10.1029/2002JD002431, in press, 2003.

Justice, C. O., J. D. Kendall, P. R. Dowty, and R. J. Scholes, Satellite remote sensing of fires during the SAFARI campaign using NOAA advanced very high resolution radiometer data, *J. Geophys. Res.*, *101*, 23,597–23,602, 1996.

Keller, M., D. J. Jacob, S. C. Wofsy, and R. C. Harriss, Effects of tropical deforestation on global and regional atmospheric chemistry, *Clim. Change*, *19*, 139–158, 1991.

Kirstine, W., I. Galbally, Y. Ye, and M. Hooper, Emissions of volatile organic compounds (primarily oxygenated species) from pasture, *J. Geophys. Res.*, *103*, 10,605–10,619, 1998.

Kliner, D. A. V., B. C. Daube, J. D. Burley, and S. C. Wofsy, Laboratory investigation of the catalytic reduction technique for measurement of atmospheric NO_y, *J. Geophys. Res.*, *102*, 10,759–10,776, 1997.

Konig, G., M. Brunda, H. Puxbaum, C. N. Hewitt, S. C. Duckham, and J. Rudolph, Relative contribution of oxygenated hydrocarbons to the total biogenic VOC emissions of selected mid-European agricultural and natural plant species, *Atmos. Environ.*, *29*, 861–874, 1995.

Koppmann, R., A. Khedim, J. Rudolph, D. Poppe, M. O. Andreae, G. Helas, M. Welling, and T. Zenker, Emissions of organic trace gases from savanna fires in southern Africa during the 1992 Southern Africa Fire Atmosphere Research Initiative and their impact on the formation of tropospheric ozone, *J. Geophys. Res.*, *102*, 18,879–18,888, 1997.

Kuhlbusch, T. A., J. M. Lobert, P. J. Crutzen, and P. Warneck, Molecular nitrogen emissions from denitrification during biomass burning, *Nature*, *351*, 135–137, 1991.

Lacaux, J. P., D. Brocard, C. Lacaux, R. Delmas, B. Ajoua, V. Yoboué, and M. Koffi, Traditional charcoal making: An important source of atmospheric pollution in the African tropics, *Atmos. Res.*, *35*, 71–76, 1994.

Lacaux, J. P., J. M. Brustet, R. Delmas, J. C. Menaut, L. Abbadie, B. Bonsang, H. Cachier, J. Baudet, M. O. Andreae, and G. Helas, Biomass burning in the tropical savannas of Ivory Coast: An overview of the field experiment Fire of Savannas (FOS/DECAFE 91), *J. Atmos. Chem.*, *22*, 195–216, 1995.

Lacaux, J. P., R. Delmas, C. Jambert, and T. A. J. Kuhlbusch, NO_x emissions from African savanna fires, *J. Geophys. Res.*, *101*, 23,585–23,596, 1996.

Lee, M., B. G. Heikes, D. J. Jacob, G. Sachse, and B. Anderson, Hydrogen peroxide, organic hydroperoxide, and formaldehyde as primary pollutants from biomass burning, *J. Geophys. Res.*, *102*, 1301–1309, 1997.

Lee, M., B. G. Heikes, and D. J. Jacob, Enhancements of hydroperoxides and formaldehyde in biomass burning impacted air and their effect on atmospheric oxidant cycles, *J. Geophys. Res.*, *103*, 13,201–13,212, 1998.

Lelieveld, J., P. J. Crutzen, D. J. Jacob, and A. M. Thompson, Modeling of biomass burning influences on tropospheric ozone, in *Fire in Southern African Savannas: Ecological and Atmospheric Perspectives*, edited by B. W. van Wilgen et al., pp. 217–238, Witwatersrand Univ. Press, Johannesburg, South Africa, 1997.

Li, Q. B., D. J. Jacob, I. Bey, R. M. Yantosca, Y. J. Zhao, Y. Kondo, and J. Notholt, Atmospheric hydrogen cyanide (HCN): Biomass burning source, ocean sink?, *Geophys. Res. Lett.*, *27*, 357–360, 2000.

Lindesay, J. A., M. O. Andreae, J. G. Goldammer, G. Harris, H. J. Annegarn, M. Garstang, R. J. Scholes, and B. W. van Wilgen, International Geosphere-Biosphere Programme/International Global Atmospheric Chemistry SAFARI-92 field experiment: Background and overview, *J. Geophys. Res.*, *101*, 23,521–23,530, 1996.

Lobert, J. M., D. H. Scharffe, W. M. Hao, T. A. Kuhlbusch, R. Seuwen, P. Warneck, and P. J. Crutzen, Experimental evaluation of biomass burning emissions: Nitrogen and carbon containing compounds, in *Global Biomass Burning: Atmospheric, Climatic, and Biospheric Implications*, edited by J. S. Levine, pp. 289–304, MIT Press, Cambridge, Mass., 1991.

Madronich, S., Photodissociation in the atmosphere, 1, Actinic flux and the effects of ground reflection and clouds, *J. Geophys. Res.*, *92*, 9740–9752, 1987.

Mason, S. A., R. J. Field, R. J. Yokelson, M. A. Kochivar, M. R. Tinsley, D. E. Ward, and W. M. Hao, Complex effects arising in smoke plume simulations due to inclusion of direct emissions of oxygenated organic species from biomass combustion, *J. Geophys. Res.*, *106*, 12,527–12,539, 2001.

Mauzerall, D. L., J. A. Logan, D. J. Jacob, B. E. Anderson, D. R. Blake, J. D. Bradshaw, B. Heikes, G. W. Sachse, H. Singh, and R. Talbot, Photochemistry in biomass burning plumes and implications for tropospheric ozone over the tropical South Atlantic, *J. Geophys. Res.*, *103*, 8401–8423, 1998.

McKenzie, L. M., W. M. Hao, G. N. Richards, and D. E. Ward, Measurement and modeling of air toxins from smoldering combustion of biomass, *Environ. Sci. Technol.*, *29*, 2047–2054, 1995.

McMillan, W. W., et al., Tropospheric carbon monoxide measurements from the Scanning High-Resolution Interferometer Sounder on 7 September 2002 in southern Africa during SAFARI 2000, *J. Geophys. Res.*, *108*, doi:10.1029/2002JD002335, in press, 2003.

Olson, J., et al., Results from the Intergovernmental Panel on Climatic Change photochemical model intercomparison (PhotoComp), *J. Geophys. Res.*, *102*, 5979–5991, 1997.

Ravishankara, A. R., and C. A. Longfellow, Reactions on tropospheric condensed matter, *Phys. Chem. Chem. Phys.*, *1*, 5433–5441, 1999.

Reid, J. S., P. V. Hobbs, R. F. Ferek, D. Blake, J. V. Martins, M. R. Dunlop, and C. Liousse, Physical, chemical, and optical properties of regional hazes dominated by smoke in Brazil, *J. Geophys. Res.*, *103*, 32,059–32,080, 1998.

Richardson, J. L., J. Fishman, and G. L. Gregory, Ozone budget over the Amazon: Regional effects from biomass burning emissions, *J. Geophys. Res.*, *96*, 13,073–13,087, 1991.

Rinsland, C. P., E. Mahieu, R. Zander, P. Demoulin, J. Forrer, and B. Buchmann, Free tropospheric CO, C_2H_6, and HCN above central Europe: Recent measurements from the Jungfraujoch station including the detection of elevated columns during 1998, *J. Geophys. Res.*, *105*, 24,235–24,249, 2000.

Schmid, B., et al., Coordinated airborne, space borne, and ground-based measurements of massive, thick aerosol layers during the dry season in South Africa, *J. Geophys. Res.*, *108*, doi:10.1029/2002JD002297, in press, 2003.

Shea, R. W., B. W. Shea, J. B. Kauffman, D. E. Ward, C. I. Haskins, and M. C. Scholes, Fuel biomass and combustion factors associated with fires in savanna ecosystems of South Africa and Zambia, *J. Geophys. Res.*, *101*, 23,551–23,568, 1996.

Singh, H. B., M. Kanakidou, P. J. Crutzen, and D. J. Jacob, High concentrations and photochemical fate of oxygenated hydrocarbons in the global troposphere, *Nature*, *378*, 50–54, 1995.

Singh, H. B., et al., Impact of biomass burning emissions on the composition of the South Atlantic troposphere: Reactive nitrogen and ozone, *J. Geophys. Res.*, *101*, 24,203–24,220, 1996.

Singh, H. B., et al., Distribution and fate of selected oxygenated organic species in the troposphere and lower stratosphere over the Atlantic, *J. Geophys. Res.*, *103*, 3795–3805, 2000.

Sinha, P., P. V. Hobbs, R. J. Yokelson, I. T. Bertschi, D. R. Blake, I. J. Simpson, S. Gao, T. W. Kirchstetter, and T. Novakov, Emissions of trace gases and particles from savanna fires in southern Africa, *J. Geophys. Res.*, *108*, doi:10.1029/2002JD002325, in press, 2003a.

Sinha, P., P. V. Hobbs, R. J. Yokelson, T. J. Christian, T. W. Kirchstetter, and R. Bruintjes, Emissions of trace gases and particles from two ships in the southern Atlantic Ocean, *Atmos. Environ.*, in press, 2003b.

Stith, J. L., L. F. Radke, and P. V. Hobbs, Particle emissions and the production of ozone and nitrogen oxides from the burning of forest slash, *Atmos. Environ.*, *15*, 73–82, 1981.

Stocks, B. J., B. W. van Wilgen, W. S. W. Trollope, D. J. McRae, J. A. Mason, F. Weirich, and A. L. F. Potgieter, Fuels and fire behavior dynamics on large-scale savanna fires in Kruger National Park, South Africa, *J. Geophys. Res.*, *101*, 23,541–23,550, 1996.

Susott, R. A., G. J. Olbu, S. P. Baker, D. E. Ward, J. B. Kauffman, and R. Shea, Carbon, hydrogen, nitrogen, and thermogravimetric analysis of tropical ecosystem biomass, in *Biomass Burning and Global Change*, edited by J. S. Levine, pp. 350–360, MIT Press, Cambridge, Mass., 1996.

Swap, R., M. Garstang, S. A. Macko, P. D. Tyson, W. Maenhaut, P. Artaxo, P. Kallberg, and R. Talbot, The long-range transport of southern African aerosols to the tropical South Atlantic, *J. Geophys. Res.*, *101*, 23,777–23,792, 1996.

Talbot, R. W., K. M. Beecher, R. C. Harriss, and W. R. Cofer III, Atmospheric geochemistry of formic and acetic acids at a mid-latitude temperate site, *J. Geophys. Res.*, *93*, 1638–1652, 1988.

Talbot, R. W., et al., Chemical characteristics of continental outflow over the tropical South Atlantic Ocean from Brazil and Africa, *J. Geophys. Res.*, *101*, 24,187–24,202, 1996.

Thompson, A. M., K. E. Pickering, D. P. McNamara, M. R. Schoeberl, R. D. Hudson, J. H. Kim, E. V. Browell, V. W. J. H. Kirchhoff, and D. Nganga, Where did tropospheric ozone over southern Africa and the tropical Atlantic come from in October 1992? Insights from TOMS, GTE TRACE A, and SAFARI 1992, *J. Geophys. Res.*, *101*, 24,251–24,278, 1996.

Trollope, W. S. W., L. A. Trollope, A. L. F. Potgieter, and N. Zambatis, SAFARI-92 characterization of biomass and fire behavior in the small experimental burns in the Kruger National Park, *J. Geophys. Res.*, *101*, 23,531–23,540, 1996.

Ward, D. E., and L. F. Radke, Emissions measurements from vegetation fires: A comparative evaluation of methods and results, in *Fire in the Environment: The Ecological, Atmospheric and Climatic Importance of Vegetation Fires*, edited by P. J. Crutzen and J. G. Goldammer, pp. 53–76, John Wiley, New York, 1993.

Ward, D. E., R. A. Susott, J. B. Kauffman, R. E. Babbitt, D. L. Cummings, B. Dias, B. N. Holben, Y. J. Kaufman, R. A. Rasmussen, and A. W. Setzer, Smoke and fire characteristics for cerrado and deforestation burns in Brazil: BASE-B Experiment, *J. Geophys. Res.*, *97*, 14,601–14,619, 1992.

Ward, D. E., W. M. Hao, R. A. Susott, R. A. Babbitt, R. W. Shea, J. B. Kauffman, and C. O. Justice, Effect of fuel composition on combustion efficiency and emission factors for African savanna ecosystems, *J. Geophys. Res.*, *101*, 23,569–23,576, 1996.

Webster, C. R., R. D. May, C. A. Trimble, R. G. Chave, and J. Kendall, Aircraft (ER-2) laser infrared absorption spectrometer (ALIAS) for in situ stratospheric measurements of HCl, N_2O, CH_4, NO_2, and HNO_3, *Appl. Opt.*, *33*, 454–472, 1994.

Worden, H., R. Beer, and C. P. Rinsland, Airborne infrared spectroscopy of 1994 western wildfires, *J. Geophys. Res.*, *102*, 1287–1299, 1997.

Yokelson, R. J., and I. T. Bertschi, Vibrational spectroscopy in the study of fires, in *Handbook of Vibrational Spectroscopy*, vol. 4, edited by J. M. Chalmers, and P. R. Griffiths, pp. 2879–2886, John Wiley, New York, 2002.

Yokelson, R. J., D. W. T. Griffith, and D. E. Ward, Open-path Fourier transform infrared studies of large-scale laboratory biomass fires, *J. Geophys. Res.*, *101*, 21,067–21,080, 1996.

Yokelson, R. J., D. E. Ward, R. A. Susott, J. Reardon, and D. W. T. Griffith, Emissions from smoldering combustion of biomass measured by open-path Fourier transform infrared spectroscopy, *J. Geophys. Res.*, *102*, 18,865–18,877, 1997.

Yokelson, R. J., D. W. T. Griffith, R. A. Susott, and D. E. Ward, Spectroscopic studies of biomass fire emissions, in *Proceedings of the 13th Conference on Fire and Forest Meteorology*, vol. 1, pp. 183–196, Int. Assoc. of Wildland Fire, Fairfield, Wash., 1998.

Yokelson, R. J., J. G. Goode, I. Bertschi, R. A. Susott, R. E. Babbitt, D. E. Ward, W. M. Hao, D. D. Wade, and D. W. T. Griffith, Emissions of formaldehyde, acetic acid, methanol, and other trace gases from biomass fires in North Carolina measured by airborne Fourier transform infrared spectroscopy (AFTIR), *J. Geophys. Res.*, *104*, 30,109–30,125, 1999.

I. T. Bertschi, Interdisciplinary Arts and Sciences, University of Washington-Bothell, Bothell, WA 59812, USA.

T. J. Christian and R. J. Yokelson (corresponding author), Department of Chemistry, University of Montana, Missoula, MT 59807, USA. (byok@selway.umt.edu)

W. M. Hao, Fire Sciences Laboratory, USDA Forest Service, Missoula, MT 59807, USA.

P. V. Hobbs, Department of Atmospheric Sciences, University of Washington, Seattle, WA 98195, USA.

D. E. Ward, Enviropyronics, LLC, P.O. Box 968, White Salmon, WA 59807, USA.